



People's Democratic Republic of Algeria
Ministry of High Education and Scientific Research



University of Chikh Laarbi Tbessi – Tébessa
Faculty of Exact Sciences and Natural Sciences

Department of Mathematics and Computer Science

Graduation Project for obtaining Master Degree.

Contribution to chest radiograph pathology categorization

Created by:

Adel SOUALMIA

Under the supervision of

The jury members:

Dr. Akram Bennour	Associate Professor	Supervisor
Dr. Houam Mohammed Yassine	Associate Professor	Examiner
Pr. Laouar Mohammed Rida	Conference Professor	President

Scholar Year: 2022/2023

Special Thanks

I thank ALLAH for giving me the strength; energy and the courage that I needed to carry for completing this work.

I would like to express my gratitude to my supervisor Dr. Bennour Akram for supporting, guiding and helping me throughout this project. Thanks to the jury members for dedicating their time to judge this work,
Thanks to anyone who participated indirectly or directly in helping to finish this work,

I also thank the professional employers' team of the Mathematics and Computer Science Faculty Department of Tebessa University,

Thanks from the bottom of my heart to every teacher who was in my academic path since 2006, the living ones and who left, May ALLAH have mercy on them...

Finally, a big thanks to my family and my friends who encouraged and supported me in my difficult times throughout this project.

Dedication

I dedicate this work to my most precious people in the world, who stayed up nights to cover us with their love,
my parents.

To my dear mother **Naziha** for her patience and supporting me in every way she could because I wouldn't be here if she wasn't here for me,
may ALLAH protect her.

To my dear father **Kamel** may ALLAH protect him.

To my sisters: **Dounia**, **Raounak** and **Razika**.

To all of my good friends.

Abstract

Classification of chest diseases is one of the most interesting research topics in recent years because it requires rapid, high-accuracy diagnosis. Although chest radiography has several advantages in diagnosing Radiologists have always been specialists in the field of diseases, but the process of understanding the image is a big problem for doctors and Radiology due to diagnostic errors made by experts in the field, and for this reason it is still the diagnostic process Somewhat confusing and difficult. This encouraged the use of modern artificial intelligence techniques such as deep learning to diagnose chest diseases and classification from the introduction of medical images and x-ray images, for this purpose began Deep learning scientists are involved in building systems based on deep learning, more precisely devolutionary neural networks. In this senior project, we have created three deep learning models based on analytical neural networks to classify some chest diseases from X-ray images. The first model is a binary classifier Related to Corona virus cases (patient/normal) achieved an accuracy rate of 99%, the second model related to inflammation Pneumonia rate of 96%, and the third model on tuberculosis with a user interface score of 98%.

ملخص

يعد تصنيف أمراض الصدر أحد أكثر موضوعات البحث إثارة للاهتمام في السنوات الأخيرة لأنه يتطلب تشخيصاً سريعاً وعالي الدقة. على الرغم من أن التصوير الشعاعي للصدر له مزايا عديدة في تشخيص الأمراض ، إلا أن عملية فهم الصورة الشعاعية كانت دائماً مشكلة كبيرة للأطباء والمختصين في مجال الأشعة بسبب أخطاء التشخيص التي يرتكبها الخبراء في المجال ، ولهذا السبب لا تزال تعد عملية التشخيص مربكة وصعبة إلى حد ما. وهذا ما شجع على استخدام تقنيات الذكاء الاصطناعي الحديثة مثل التعلم العميق لتشخيص أمراض الصدر والتصنيف من إدخال الصور الطبية وصور الأشعة السينية، لهذا الغرض بدأ علماء التعلم العميق في بناء أنظمة قائمة على التعلم العميق ، و بشكل أدق الشبكات العصبية الالتفافية. في مشروع التخرج هذا ، أنشأنا ثلاثة نماذج تعليمية عميقة تعتمد على الشبكات العصبية الالتفافية التي تم تدريبها لتصنيف بعض أمراض الصدر من صور الأشعة السينية ، النموذج الأول عبارة عن مصنف ثنائي يتعلق بحالات فيروس كورونا (مريض/ عادي) حقق نسبة دقة 99% ، النموذج الثاني يتعلق بالالتهاب الرئوي بنسبة 96% ، والنموذج الثالث حول مرض السل مع واجهة مستخدم حقق 98%.

Table of Contents:

Abstract.....	I
ملخص.....	II
Table of Contents.....	III
List of Figures.....	IV
List of Tables.....	V
General Introduction.....	1
Chapter 1: Theoretical Study about chest diseases and medical imaging.....	2
1/Introduction.....	3
2/overview about chest diseases.....	3
2.1/Types of some chest diseases.....	3
2.2.1/Pneumonia.....	3
2.2.2/Tuberculosis.....	4
2.2.3/Covid-19.....	5
3/overview about medical imaging.....	6
4/conclusion.....	9
Chapter 2: Artificial Intelligence Technics.....	10
Introduction.....	11
1/Artificial Intelligence Definition.....	11
2/Machine learning Definition.....	12
3/Types of Machine Learning.....	12
3.2.1/Supervised Learning.....	12
3.2.2/Unsupervised Learning.....	13
3.2.3/Reinforcement Learning.....	14
4/Artificial Neural Networks.....	15
4.1/Definition.....	15
4.2/Perceptron.....	16
4.3/Activation Functions.....	17
4.1/Binary step.....	17
4.2/Linear.....	18
4.3/Rectified Linear Unit.....	19
4.4/Sigmoid/Logistic.....	20
5/Deep Learning Definition.....	20
6/Difference between Machine Learning and Deep Learning.....	20
7/Deep learning types.....	21
6.1/Recurrent Neural Networks.....	21

6.2/Convolutional Neural Networks.....	22
8/Convolutional Neural Networks prototypes (Keras Applications)	23
8.1/VGGNet.....	24
8.2/ResNet.....	26
8.3/GoogLeNet.....	26
11/Conclusion.....	28
Chapter 3: State of theArt.....	29
1/Introduction.....	30
2/Related Works.....	30
2.1/T. Wang, J. Li, G. Xia, et al (2021)	30
2.2/Y. Tang, L. Zhang, Y. Gao, et al. (2018)	30
2.3/A. Rajpurkar, C. Irvin, K. Zhu, et al. (2018)	31
2.4/M. Minaee, Y. Kafieh, and R. Sonka (2021)	31
2.5/S. B. Park, H. K. Kim, and H. Kim (2019)	31
2.6/A. Anthimopoulos, S. Christodoulidis, L. Ebner, et al.	32
2.7/W. Dou, L. Gao, Y. Zhu, et al. (2017)	33
2.8/K. J. Lee, H. S. Kim, and Y. S. Lee (2018)	33
2.9/J. R. Neyman, J. A. Guo, and R. A. Bhavsar (2021)	34
2.10/Kim, S. Lee, S. Lee, et al. (2021):	35
2.11/Dataset Definition.....	40
2.12/Used Approach.....	41
3/Conclusion.....	42
Chapter 4: Concept and programming.....	43
1/Introduction.....	44
2/Work Environment and tools.....	44
2.1/Google Colaboratory.....	44
2.2/Python Language (Tools and Libraries)	44
2.2.1/Gradio.....	45
2.2.2/NumPy.....	45
2.2.3/MatPlotLib.....	46
2.2.4/Pandas.....	47
2.2.5/Sickit-Learn.....	48
2.2.6/TensorFlow.....	48
2.2.7/Keras.....	48
3/General Architecture.....	49
3.1/used Datasets.....	49
3.2.1/Data preprocessing.....	50
Used Splitting Method.....	51

3.2/Models Evaluation.....	52
3.2.2.1/Classification Performance Metrics.....	52
3.2.2.2/Confusion Matrix.....	53
3.3/Models Architecture.....	53
4/Programming.....	57
4.1/Mount google drive in google colab.....	57
4.2/importing libraries.....	59
4.3/Dataset Access and Augmentation Method.....	60
4.4/Models training.....	60
5/Experiments and Results.....	60
5.1/Graphic presentation.....	60
5.2/Models Evaluation.....	61
5.3/Comparing results with the State-of-the-art.....	67
6/Conclusion.....	68
General Conclusion.....	69
Bibliography.....	70

List of Figures:

Figure 1: Pneumonia.....	4
Figure 2: Tuberculosis X-Ray.....	4
Figure 3: Tuberculosis.....	5
Figure 4: Covid 19 shape.....	5
Figure 5: Covid 19 X-Ray.....	6
Figure 6: Medical Imaging procedure.....	7
Figure 7: Artificial Intelligence.....	11
Figure 8: Supervised Machine Learning.....	13
Figure 9: Unsupervised Machine Learning.....	14
Figure 10: ReInforcement Learning.....	15
Figure 11: Artificial Neural Network Structure.....	16
Figure 17: Multilayer Perceptron.....	16
Figure 12: Binary step Activation Function.....	17
Figure 13: Linear Activation Function.....	18
Figure 14: Rectified Linear unit activation Function.....	19
Figure 15: Sigmoid Activation Function.....	20
Figure 16: Machine Learning vs. deep Learning.....	21
Figure 18: Reccurent Neural Network.....	22
Figure 19: Convolutional Neural Network Layers.....	23
Figure 20: keras Applications.....	24
Figure 21: keras VGG16.....	25
Figure 22: keras VGG19.....	25
Figure 23: ResNet.....	26
Figure 24: GoogLeNet.....	27
Figure 25: Google Colaboratory.....	36
Figure 26: Python.....	37
Figure 27: Gradio.....	42
Figure 28: Numpy.....	44
Figure 29: Matplotlib.....	45
Figure 30: Pandas.....	45
Figure 31: SkLearn.....	46
Figure 32: Tensorflow.....	46
Figure 33: keras.....	47
Figure 34: General overview.....	47
Figure 35: Base Model 1.....	48
Figure 36: Base Model 2.....	48
Figure 37: Base Model 3.....	49
Figure 38: Access google drive method 1.....	54
Figure 39: Access google drive method 2.....	55

Figure 40: Drive permission window.....	56
Figure 41: Importing libraries.....	57
Figure 42: Data access.....	57
Figure 43: Data reshape.....	58
Figure 44: training and testing	59
Figure 45: Accuracy and Loss of Model 1.....	60
Figure 46: Accuracy and Loss of Model 2.....	60
Figure 47: Accuracy and Loss of Model 3.....	60
Figure 48: Model 1 Evaluation score.....	61
Figure 48.1: Model 2 Evaluation score.....	61
Figure 59: Model 3 Evaluation score.....	62
Figure 50: graphical user interface 1.....	63
Figure 51: graphical user interface 2.....	65
Figure 52: graphical user interface 3.....	65

List of Tables:

Table 1: State-of-The-Art Summary	34
Table 2: confusion Matrix Architecture.....	40
Table 3: Model 2 confusion Matrix.....	50
Table 4: Model 3 confusion Matrix.....	51
Table 5: Results summary.....	54
Table 6: comparing results.....	54

General Introduction:

Medical imaging is an important tool in the diagnosis and treatment of various medical conditions and diseases. However, analyzing medical images can be challenging and time-consuming, requiring specialized knowledge and expertise. In recent years, Medical image analysis has benefited from the precision and efficacy that AI techniques like machine learning and deep learning have improved. [1].

AI algorithms have the capacity to analyze large volumes of medical imaging data and identify patterns and features that may be difficult for human experts to detect [2]. By training these algorithms on extensive medical imaging data, they can learn to recognize specific features and abnormalities that indicate different diseases and medical conditions. This can result in earlier and more accurate diagnoses, personalized treatment plans, and improved patient outcomes.

Furthermore, AI techniques can also help to reduce the workload of healthcare professionals by automating routine tasks and providing decision support. For example, AI algorithms can assist radiologists in detecting and classifying abnormalities in medical images, allowing them to focus on more complex cases or to prioritize urgent cases.

The application of AI to medical imaging has the potential to revolutionize the field of radiology and raise the bar for patient care. The main goal of this study is to use convolutional neural network models to classify radiographs of chest infections. By doing this, radiologists and medical professionals can more precisely identify and categorize pulmonary diseases from chest X-rays, improving patient outcomes and diagnostic accuracy.

This memory is structured as follows:

Chapter (1): This chapter presents a theoretical study on a group of common lung diseases and overview about medical imaging types.

Chapter (2): This chapter contains several AI technologies, in particular the techniques on which the study is based, such as deep learning and convolutional neural networks.

Chapter (3): In this chapter, we describe a group of related works and show their results to compare them with our work.

Chapter (4): This chapter describes the design of our contribution that corresponds to a deep neural network architecture for the classification of several diseases on X-ray images.

Chapter 1: Theoretical Study on Medical Imaging And Chest Diseases

1. Introduction:

Lungs represent an essential role in the human body because they work continuously throughout its life, from birth to death in order to provide the body with the oxygen, which is taken from the external environment. Since the lungs are in relation to the External environment, they are sensitive to many diseases that we will discuss in this chapter, we'll also talk about the main types of medical images that will help in the diagnosis or identifying these diseases.

2. Overview about chest diseases

Chest diseases are among the most prevalent conditions worldwide, with millions of individuals suffering from lung diseases in the United States alone. These diseases are typically caused by smoking, infections, and genetic factors. The lungs play a vital role in the complex process of breathing, involving the expansion and contraction of thousands of muscles numerous times daily to inhale oxygen and exhale carbon dioxide. Any malfunction in the human body system can lead to lung disease. [3]

2.1 Types of some chest diseases:

- **2.2.1.Pneumonia:**

Lung health is seriously threatened by the respiratory infection pneumonia. The process of breathing normally fills the lungs' alveoli with air in healthy people who have no underlying medical conditions. However, in cases of pneumonia, the alveoli may swell with pus and fluid, creating breathing difficulties and a reduction in oxygen availability.

Unfortunately, pneumonia continues to be the leading infectious cause of death in children worldwide. Surprisingly, pneumonia killed 740,180 children under the age of five in 2019 alone, accounting for 14% of all deaths in this age group [4]. In addition, pneumonia causes 22% of deaths in children from 1 to 5 years old. South Asia and sub-Saharan Africa account for the majority of pneumonia-related fatalities.

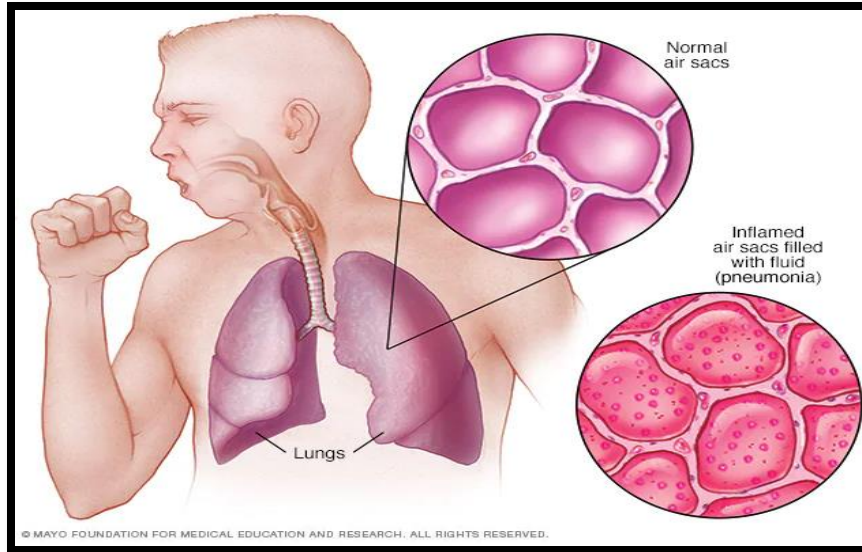


Figure 1: Pneumonia [4].

- **2.2.2. Tuberculosis:**

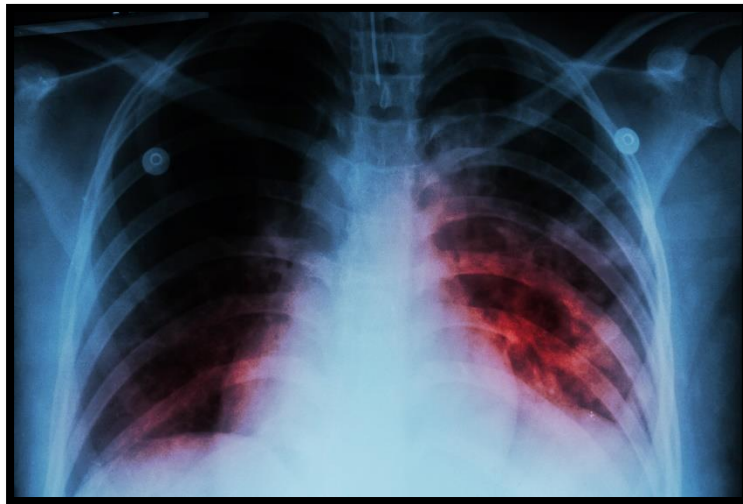


Figure 2: Tuberculosis X-Ray [5]

Tuberculosis is a persistent (chronic) advancing mycobacterial infection frequently has an asymptomatic latency period following the initial infection. Lungs are the organs most typically impacted by tuberculosis. A productive cough, a fever, weight loss, and a general sensation of unwellness are symptoms. Sputum smear, culture,

And, if applicable, nucleic acid amplification tests are the primary methods used for diagnosis. Antimicrobial medication combinations that are taken consistently for at least 4 months are the basis of treatment.

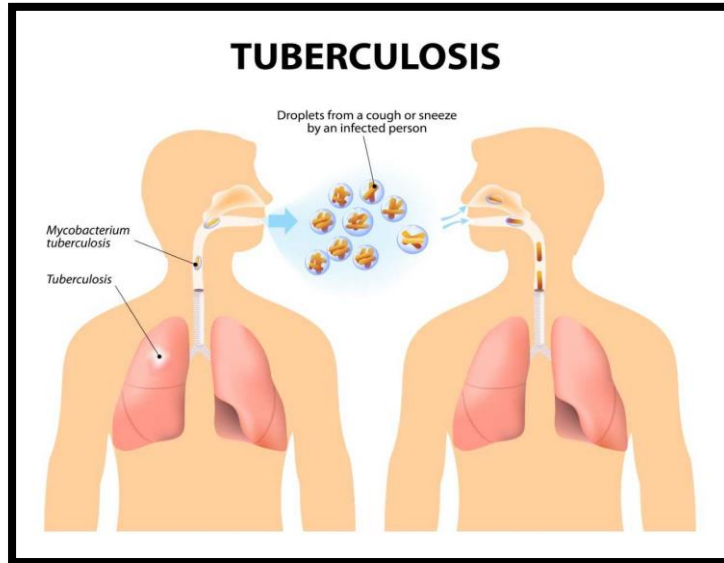


Figure 3: Tuberculosis [6].

- **2.2.3. Covid-19**

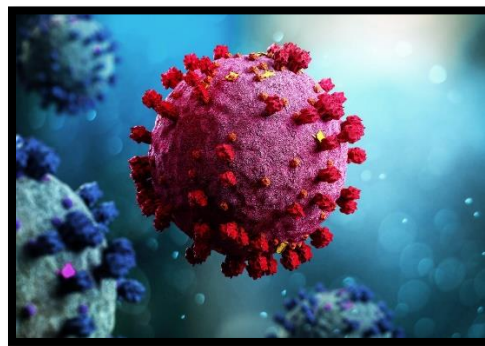


Figure 4: Covid-19 shape [7]

COVID-19 is a respiratory illness caused by the SARS-Coronavirus-2 virus, and while most people who contract the virus experience mild to moderate symptoms and recover without needing medical attention, a small percentage may develop severe symptoms that require medical care. People who are older or have underlying health conditions, such as cancer, diabetes, chronic respiratory disease, or cardiovascular disease, are more likely to experience severe illness from COVID-19

Although anyone can become ill from COVID-19, regardless of age, it is not accurate to say that everyone who contracts the virus will suffer terribly or die from it. The case fatality rate for COVID-19 is estimated to be around 2-3%, but this can vary depending on a number of factors. COVID-19 can cause a range of symptoms beyond respiratory illness, such as fever, fatigue, body aches, and loss of taste or smell. To reduce the spread of the virus and protect against severe illness, it is recommended to follow preventative measures such as vaccination, wearing masks, practicing physical distancing, and good hand hygiene. [8]

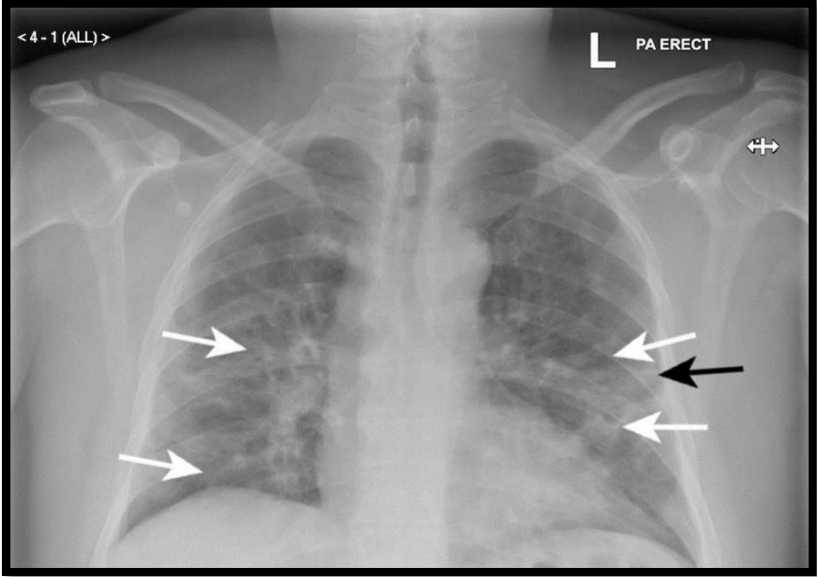


Figure 5: Covid-19 X-Ray [9].

3. Overview about medical imaging

Medical imaging, also known as radiography, is a field of medicine where doctors create various images of body parts for diagnostic or therapeutic purposes. Through the use of non-invasive techniques, medical imaging allows clinicians to make non-intrusive diagnoses of illnesses and injuries. [10]



Figure 6: Medical Imaging Procedure [11].

For diagnostic reasons, medical imaging makes use of "invisible" waves like electromagnetic radiation, magnetic fields, or sound waves. These waves are produced from a source positioned on one side of the body, pass through the body and the area of interest, and are then picked up by a sensor positioned on the other side. Different bodily tissues absorb the waves in different ways, creating a picture made up of the "shadows" of those tissues. Modern medical imaging systems provide direct digital image capture and monitor viewing in contrast to traditional medical imaging methods that depended on photo detector plates that needed film processing. [7].

A key component of the better outcomes of contemporary medicine is medical imaging, and it has many types, which listed as follows:

- X-rays:
- Magnetic Resonance imaging (MRI)
- Ultrasounds
- Tactile Imaging
- Computerized Tomography (CT scan).

3.1. X-Ray:

X-rays are a widely used imaging technique that utilizes electromagnetic radiation to visualize internal structures of the body. X-ray imaging involves passing a focused beam of X-ray radiation through the body, and the resulting image provides information about the density and composition of tissues. X-rays are particularly

useful for examining bones, detecting fractures, and identifying abnormalities in the lungs and other organs.

3.2. Magnetic Resonance imaging (MRI):

MRI is a non-invasive imaging technique that utilizes a strong magnetic field and radio waves to generate detailed images of the body's internal structures. It provides high-resolution images by measuring the response of hydrogen atoms in tissues to the magnetic field. MRI is particularly useful for evaluating soft tissues, such as the brain, spinal cord, muscles, and joints, and is widely used in diagnosing various medical conditions.

3.3. Ultrasound:

Ultrasound imaging, also known as sonography, uses high-frequency sound waves to create real-time images of internal structures. Ultrasound waves are emitted by a transducer and bounce back when they encounter different tissues, generating images based on the echoes. This imaging technique is commonly used to visualize organs, blood vessels, and the developing fetus during pregnancy.

3.4. Tactile Imaging:

Tactile imaging, also referred to as palpation or touch imaging, involves the manual examination of the body to assess structures and detect abnormalities. It relies on the sense of touch to evaluate the texture, size, and consistency of tissues. Tactile imaging is commonly used in clinical examinations, such as breast exams and lymph node assessments.

3.5. Computerized Tomography:

CT scan, also known as computed tomography, combines X-rays with advanced computer processing to create cross-sectional images of the body. It involves rotating an X-ray source and detector around the patient, capturing multiple X-ray images from different angles. The computer then reconstructs these images to create detailed cross-sectional views. CT scans are valuable for diagnosing various conditions and are particularly useful for evaluating the brain, chest, abdomen, and pelvis.

4. Conclusion:

In this chapter, we talked about lungs of the body and their function in the human system, also the most prevalent illnesses that affect them.

We talked about the medical imaging in general and some of the medical picture types.

Chapter 2: Artificial Intelligence Technics

1. Introduction

With the increasing significance of Artificial Intelligence (AI) in numerous areas of development, such as health, sports, food, commerce, and industry, it has started to revolutionize the world. However, there are still many individuals who lack understanding of this subject. Hence, this chapter aims to provide a comprehensive overview of artificial intelligence, its definition, and commonly used technologies. [12].

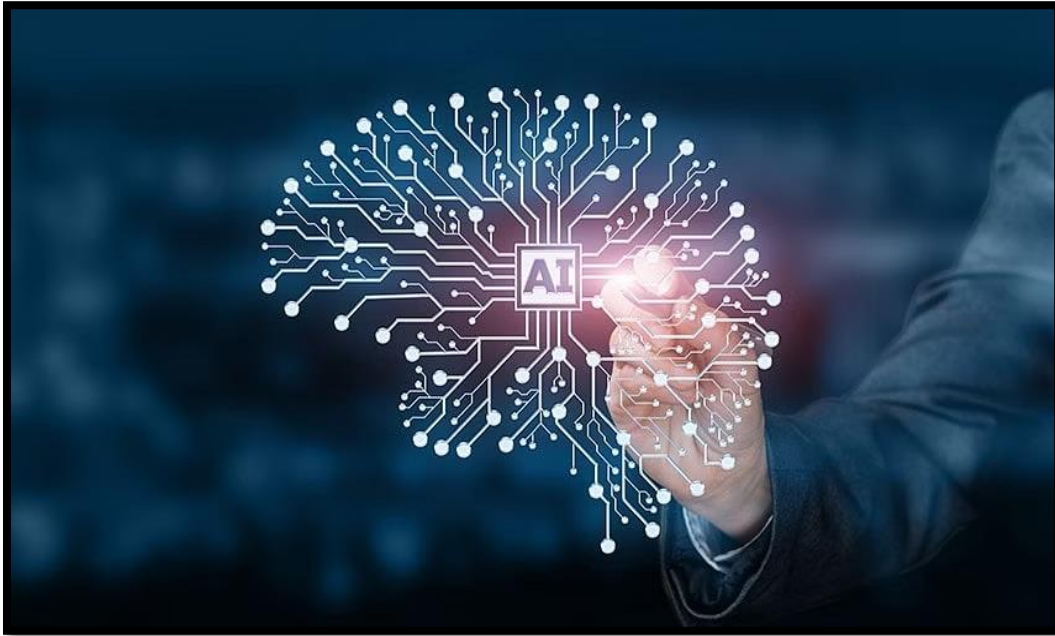


Figure 7: Artificial Intelligence Graphic Design [13]

2. Definition

The ability of a machine to display intellect in contrast to that of humans and other animals is referred to as artificial intelligence (AI). This encompasses tasks like speech recognition, input mapping, computer vision, and translation into natural languages. A few of the numerous real-world applications of AI include intelligent web search engines like Google Search, recommendation engines used by YouTube, Amazon, and Netflix, speech recognition tools like Siri and Alexa, self-driving cars like Waymo, artistic software like ChatGPT and AI art, automated decision-making, and tactical game systems like chess and Go. The AI impact refers to the possibility that as robots advance, certain tasks that were once considered to need "intelligence" may no longer fall under this category. Optical character recognition is one such widely used technique. [14].

3. Machine Learning:

3.1. Definition:

The practice of developing algorithms to find patterns and trends in previous data, which may subsequently be used to forecast future data, is known as machine learning. A growing number of academics and medical experts are using machine learning techniques to develop and evaluate tools that will help in the diagnosis and treatment of individuals with brain illnesses [15] A recent evaluation of these techniques' applications to the treatment of neurological and psychiatric illnesses that impact the brain can be found in Machine Learning: Techniques and Applications to Brain Diseases. This book is intended for a non-technical readership that consists of neuroscientists, psychologists, psychiatrists, neurologists, and other healthcare providers.

3.2. Types

There is three general Machine Learning types of which we can mention Supervised Learning and Unsupervised Learning and reinforcement learning.

3.2.1. Supervised Learning:

A training set is used in supervised learning to direct models toward the desired results. This training dataset contains the necessary input data and outputs, enabling the model to gradually improve its comprehension. The algorithm's accuracy is measured using the loss function, and iterations are carried out until the error is sufficiently minimized. [16]

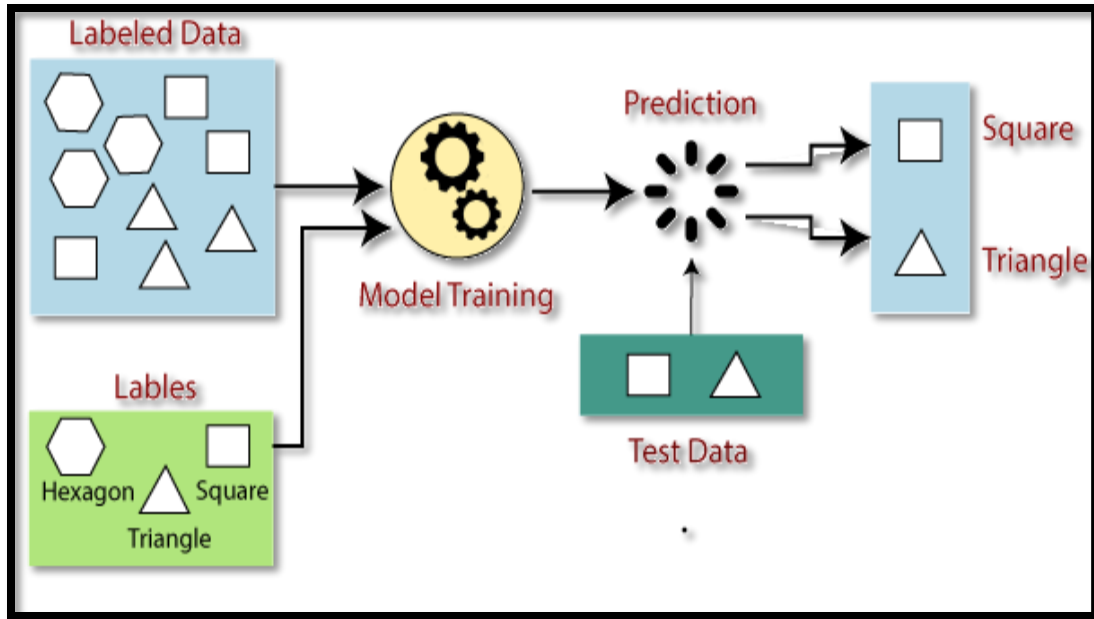


Figure 8: Supervised Machine Learning schema [17]

3.2.2. Unsupervised Learning:

Without the aid of a human, an algorithm is used to evaluate and organize unlabeled data in a sort of machine learning called "unsupervised learning". This technique is useful for identifying hidden patterns or clusters within data, as it can discover similarities and differences in information without relying on pre-existing labels. Applications of unsupervised learning include exploratory data analysis, customer segmentation, and image recognition. [18]

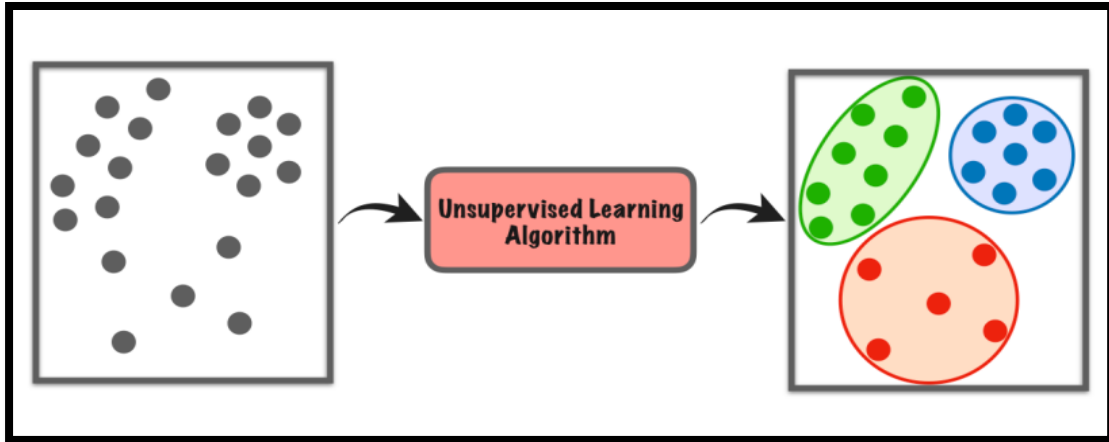


Figure 9: Unsupervised Machine Learning schema [19]

3.2.3. Reinforcement learning:

Reinforcement Learning (RL) is a type of machine learning focused on decision-making. Its objective is to learn the best behavior in a particular environment to obtain maximum reward. RL accomplishes this by interacting with the environment and observing its responses, similar to how a child explores their surroundings to learn the actions that lead to a desired outcome.

In contrast to supervised learning, RL does not rely on pre-labeled data. Instead, the algorithm must independently discover the sequence of actions that lead to maximum reward. This process involves a trial-and-error approach, where the quality of actions is measured not only by the immediate reward they return but also by the potential delayed reward they may generate.

Reinforcement learning is a powerful algorithm that can learn to take the right actions in an unfamiliar environment without the guidance of a supervisor. It has been successfully applied in various fields, such as robotics, game playing, and autonomous vehicle navigation. [20].

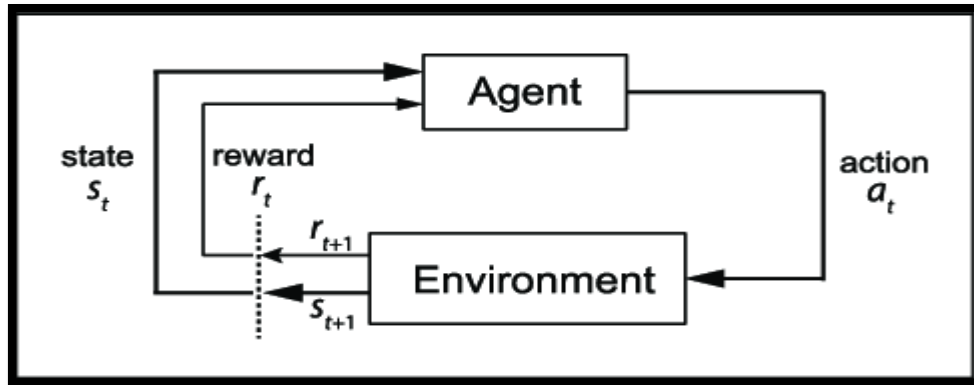


Figure 10: Reinforcement Learning Schema [21]

1. Artificial Neural Networks:

Computer architecture known as Artificial Neural Networks (ANNs) is modeled after the neural networks in the human brain. Artificial neurons in ANNs perform brain-like functions as do biological neurons. Each neuron is linked to its neighbors neurons by edges that can transmit messages to other cells. The strength of the connections between neurons increases as the network learns through a process known as training. Each neuron's output is dictated by a non-linear function of the sum of its inputs. Applications for ANNs include audio and picture recognition, natural language processing, and predictive analytics. [22].

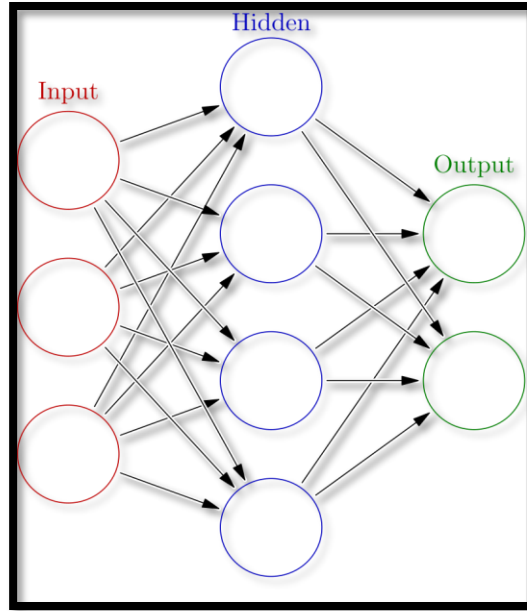


Figure 11: Artificial Neural Network Structure [23]

2. Multilayer Perceptron:

An input, output, and hidden layer feed-forward neural network is referred to as a multi-layer perceptron (MLP). The hidden layers, which perform the computational operations, receive the input signal from the input layer. Receiving signals from the hidden layers, the output layer carries out crucial tasks like prediction or classification. As data moves from the input layer to the output layer, the MLP computes. The backpropagation learning technique is used to train the neurons in the MLP. MLPs have the ability to approximate any continuous function and can solve problems that are not linearly separable. Pattern categorization, recognition, prediction, and approximation are some of the main uses of MLP [24].

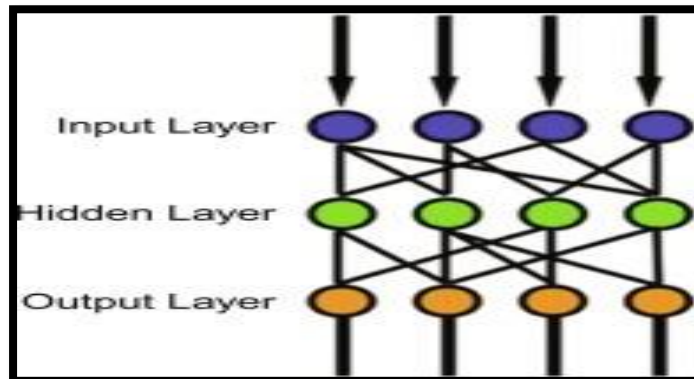


Figure 17: MultiLayer Perceptron schema [25]

3. Activation funCtions

The activation function in a neural network determines if a neuron should be activated based on its input. It helps in deciding if the neuron's input is significant for the prediction process, using simple mathematical operations. Its primary function is to generate the output based on a set of input values that are fed into a node [26], there are many activation functions we will see some of them below:

3.1. Binary Step:

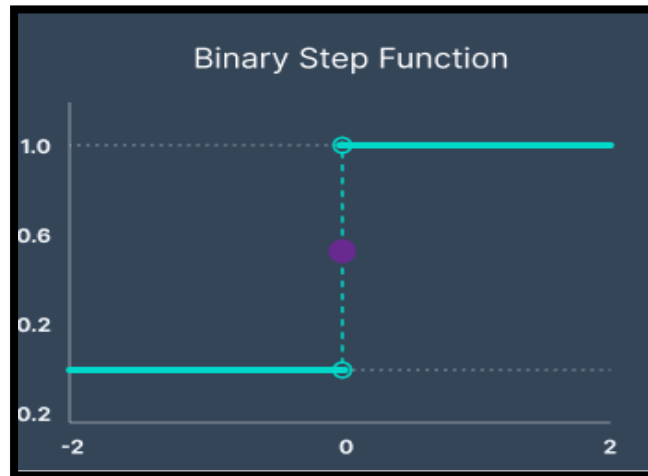


Figure 12: Binary Step Activation Function [27]

As shown in figure 17 above, the binary step is an activation function that works on the threshold-based activation concept. The neuron is activated when the input value reaches a particular threshold; otherwise, it is deactivated. Typically, the threshold value is set to zero. This form of activation function is appropriate for binary classification issues with one of two output classes. It cannot, however, be used for multi-class classification jobs. [28]

3.2. Linear

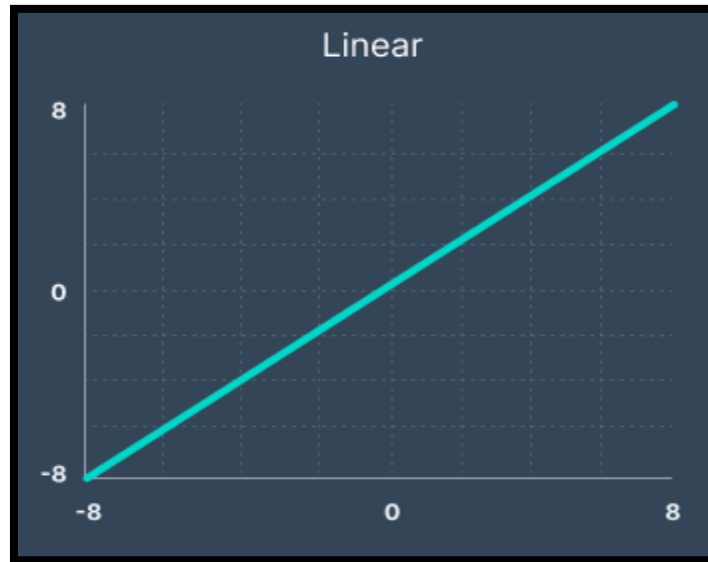


Figure 13: Linear Activation Function [29]

In this activation function, the output is directly proportional to the sum of the weighted neurons. Unlike the Binary Step function, the Linear Activation function can be used for multi-class classification tasks. However, it has some limitations. In back-propagation, changes made are constant, which is not suitable for learning. Additionally, the function has a major drawback; no matter how many layers a neural network has, the last layer will always be dependent on the first layer. This limitation reduces the neural network's capacity to handle complex problems. [30].

3.3. Rectified Linear Unit Activation Function:

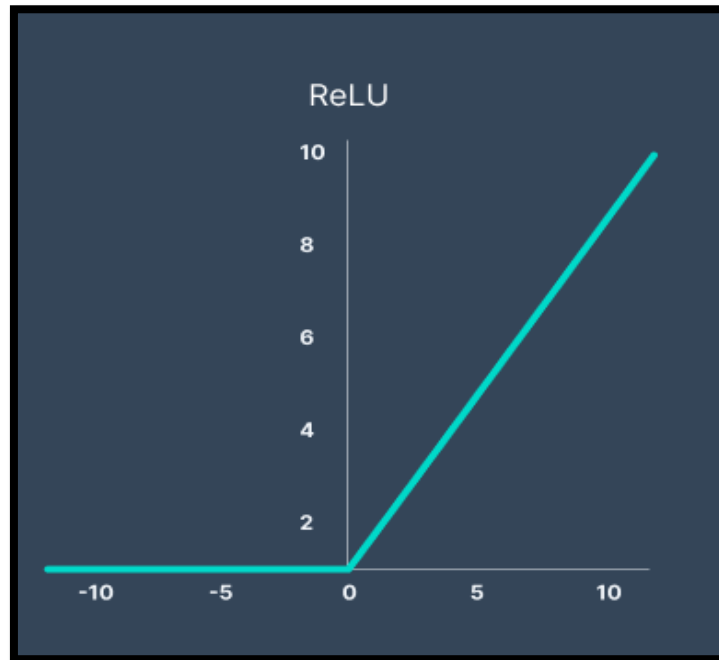


Figure 14: Rectified Linear Unit Activation Function [31]

The ReLU activation function has a potential issue known as the "dying ReLU" problem. For positive inputs, the output of the function can range from zero to infinity. However, for negative inputs or zero, the output is always zero, which can hinder the backpropagation process. [32]

3.4. Sigmoid/Logistic:

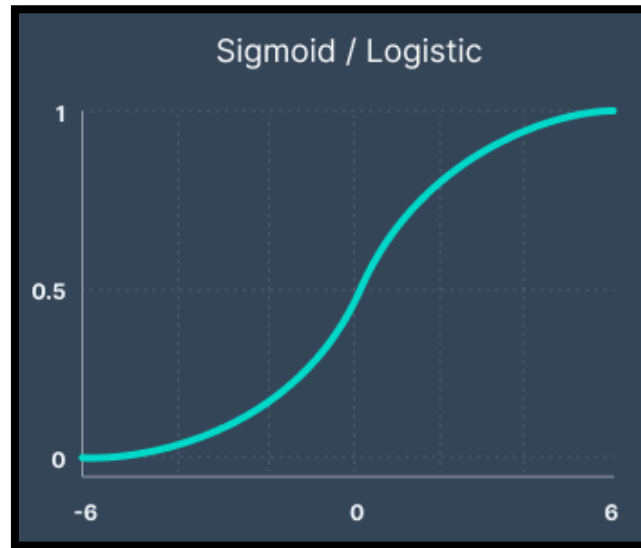


Figure 15: Sigmoid Activation Function [33]

The sigmoid function, also called the logistic function, is an activation function that returns an output ranging from 0 to 1, which is useful for normalizing the output of each neuron. However, the sigmoid function can cause the neural network to stop learning when input values are extremely high or low, resulting in the vanishing gradient problem. [34].

4. Deep Learning Definition:

Deep learning is a subset of machine learning that uses neural networks with numerous layers to analyze intricate data. The architecture of deep learning models is based on artificial neurons that aim to imitate the functioning of the human brain. The use of multiple layers of neurons in deep learning models enables them to extract and learn high-level features from massive datasets. This approach can be applied in various domains such as image recognition, natural language processing, and predictive modeling. [35]

5. Difference between machine learning and deep learning:

Artificial intelligence (AI) is divided into the areas of machine learning and deep learning. AI that can self-adjust with little assistance from humans is referred to as machine learning. Deep learning, on the other hand, is a subset of machine learning that uses artificial neural networks to mimic the way the human brain learns.

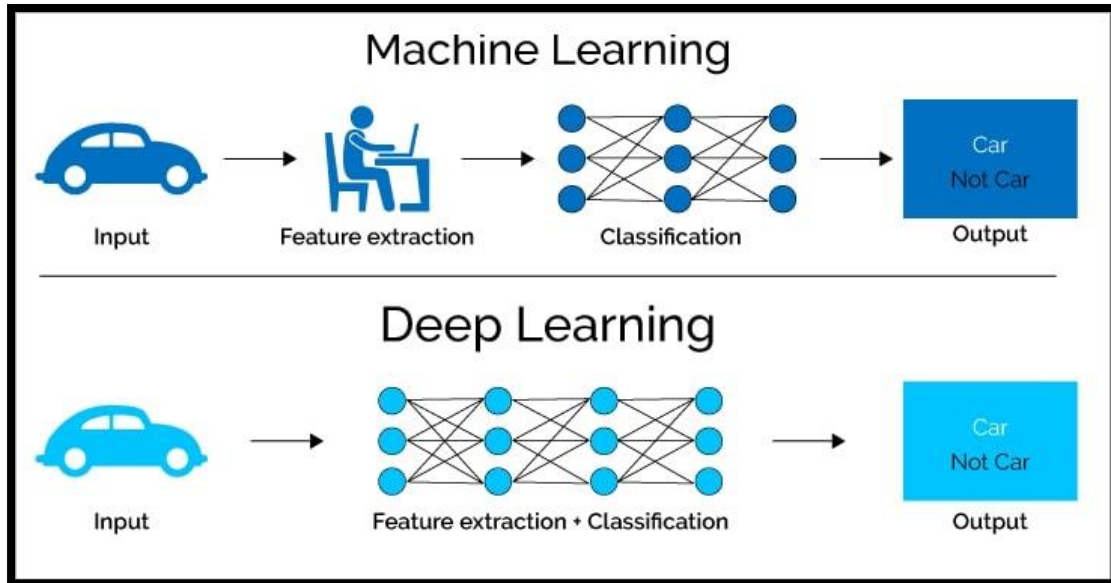


Figure 16: Machine Learning vs. Deep Learning [36].

6. Major Deep Learning Types:

There are three main types of deep learning, which included as:

- MLP: which stands for Multilayer Perceptron
- RNN: stands for Recurrent Neural Networks
- CNN: stands for Convolutional Neural Networks

6.1. Recurrent Neural Network:

Recurrent neural networks are a type of ANN which use sequential time-series data. Their functions can be used for tasks involving speech recognition, natural language processing, and image captioning and language translation. Unlike traditional neural networks, Recurrent Neural Networks have a memory which allow them to influence the input and output using information from previous inputs. [37]

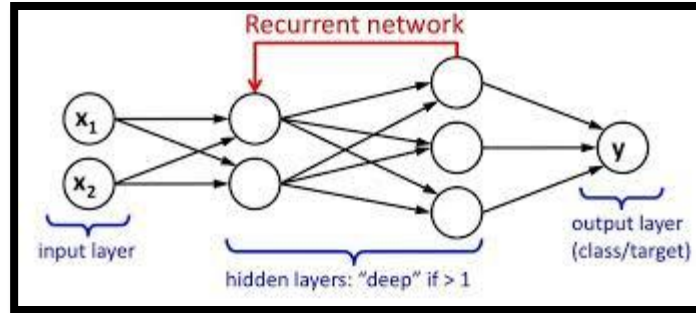


Figure 18: Recurrent Neural Network schema [38]

6.2. Convolutional Neural Networks (CNN):

A deep learning approach used for image identification and classification is a convolutional neural network (CNN). From input photos, it is intended to learn spatial hierarchies of features in an automatic and adaptive manner, without requiring manual feature extraction. The key idea behind CNNs is to use convolution operations on the input image, which allows the network to learn filters that capture important patterns and features in the image. By stacking multiple convolutional layers and other types of layers, such as pooling and activation layers, CNNs can learn increasingly complex features and patterns, leading to highly accurate image recognition and classification. [39]

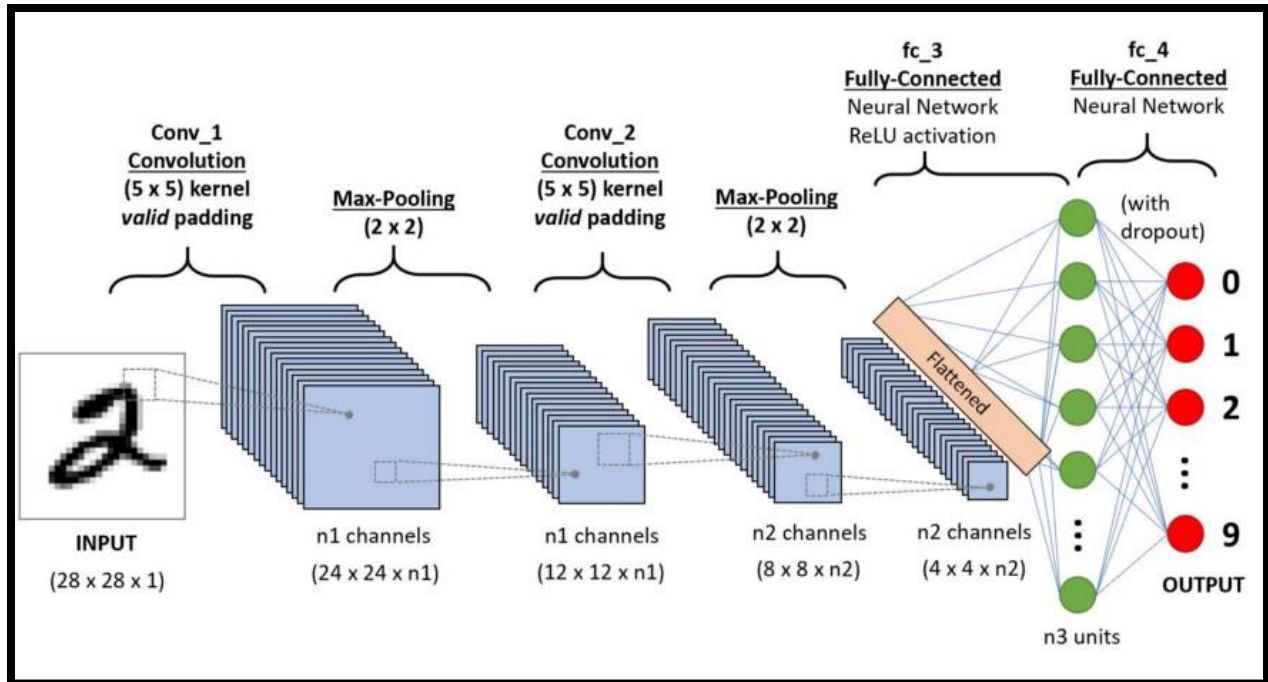


Figure 19: Convolutional Neural Network Layers [40]

7. Keras Applications:

There is a lot of pretrained Models used for Image classification in Keras, the official Table from keras website below contains a few;

Available models							
Model	Size (MB)	Top-1 Accuracy	Top-5 Accuracy	Parameters	Depth	Time (ms) per inference step (CPU)	Time (ms) per inference step (GPU)
Xception	88	79.0%	94.5%	22.9M	81	109.4	8.1
VGG16	528	71.3%	90.1%	138.4M	16	69.5	4.2
VGG19	549	71.3%	90.0%	143.7M	19	84.8	4.4
ResNet50	98	74.9%	92.1%	25.6M	107	58.2	4.6
ResNet50V2	98	76.0%	93.0%	25.6M	103	45.6	4.4
ResNet101	171	76.4%	92.8%	44.7M	209	89.6	5.2
ResNet101V2	171	77.2%	93.8%	44.7M	205	72.7	5.4
ResNet152	232	76.6%	93.1%	60.4M	311	127.4	6.5
ResNet152V2	232	78.0%	94.2%	60.4M	307	107.5	6.6
InceptionV3	92	77.9%	93.7%	23.9M	189	42.2	6.9
InceptionResNetV2	215	80.3%	95.3%	55.9M	449	130.2	10.0
MobileNet	16	70.4%	89.5%	4.3M	55	22.6	3.4
MobileNetV2	14	71.3%	90.1%	3.5M	105	25.9	3.8
DenseNet121	33	75.0%	92.3%	8.1M	242	77.1	5.4
DenseNet169	57	76.2%	93.2%	14.3M	338	96.4	6.3
DenseNet201	80	77.3%	93.6%	20.2M	402	127.2	6.7
NASNetMobile	23	74.4%	91.9%	5.3M	389	27.0	6.7
NASNetLarge	343	82.5%	96.0%	88.9M	533	344.5	20.0
EfficientNetB0	29	77.1%	93.3%	5.3M	132	46.0	4.9
EfficientNetB1	31	79.1%	94.4%	7.9M	186	60.2	5.6
EfficientNetB2	36	80.1%	94.9%	9.2M	186	80.8	6.5

Figure 20: keras applications (from keras.io)

7.1. VGGNet

The Visual Geometry Group (VGG) at the University of Oxford has devised the convolutional neural network architecture known as VGGNet. The deep layer

structure of the VGGNet architecture—up to 19 layers in certain versions—is well-known. The network design is composed of pooling layers first, then repeated convolutional layers, and finally fully linked layers. In order to accomplish related works performance on picture classification activities, deeper architectures are essential, as proved by VGGNet, and this insight has sparked the construction of even deeper networks in the years thereafter. [41]

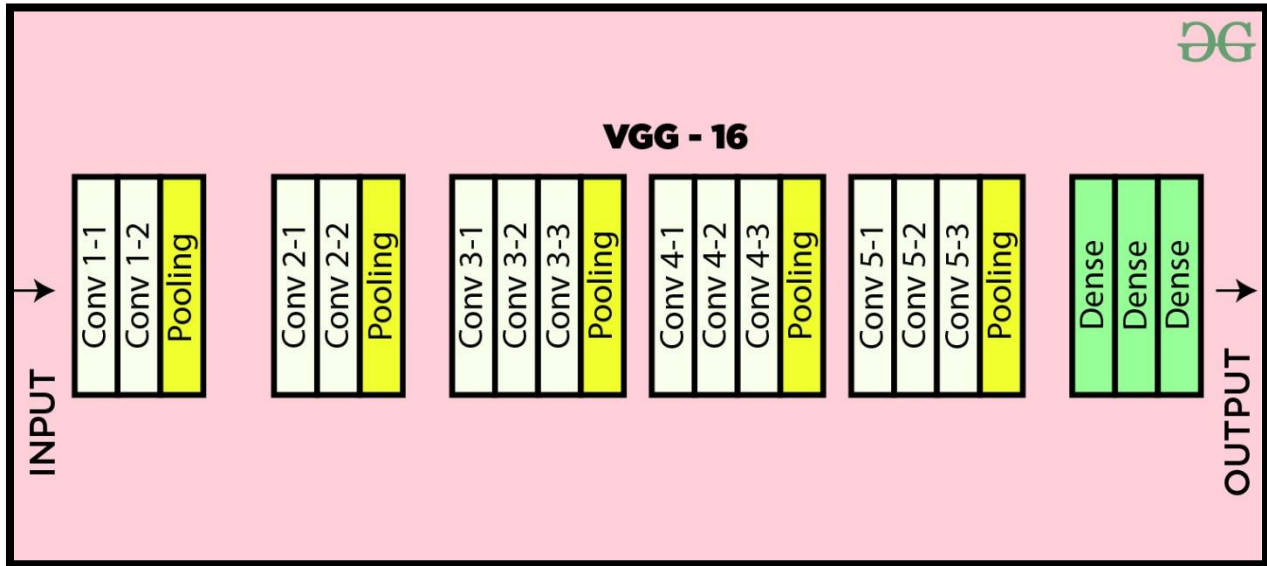


Figure 21: Keras VGG16 Architecture [42]

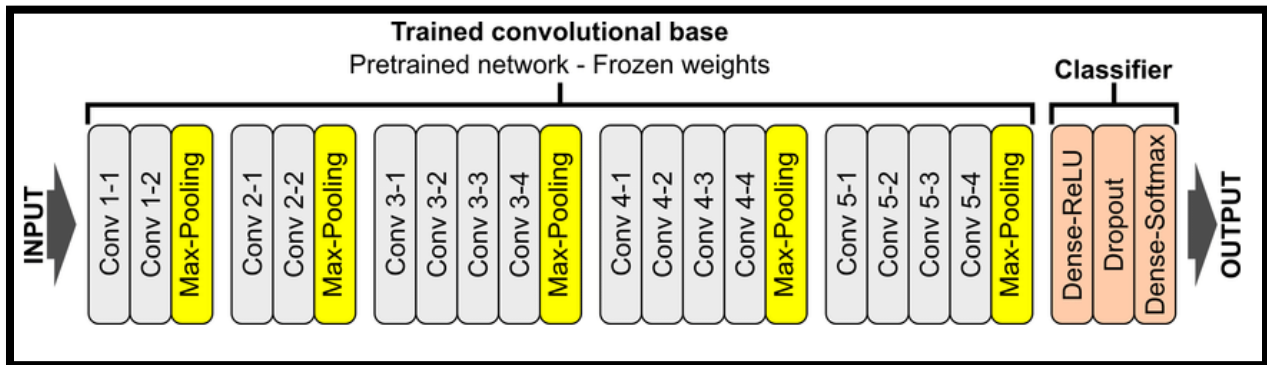


Figure 22: Keras VGG19 Architecture [43]

7.2. ResNet

The deep learning architecture known as ResNet, or "Residual Network," enables the formation of extremely deep neural networks. It makes use of skip connections to overcome vanishing gradient issues that would otherwise prevent deep neural networks from being successfully trained. ResNet can reduce information loss and enable more effective and precise training of deeper networks by omitting some layers from the training process. The network may learn residual functions thanks to the identity mappings added by the skip connections, which is where the term "Residual Network" originates. ResNet has been effectively used for a variety of applications, including segmentation, object identification, and picture categorization. [44].

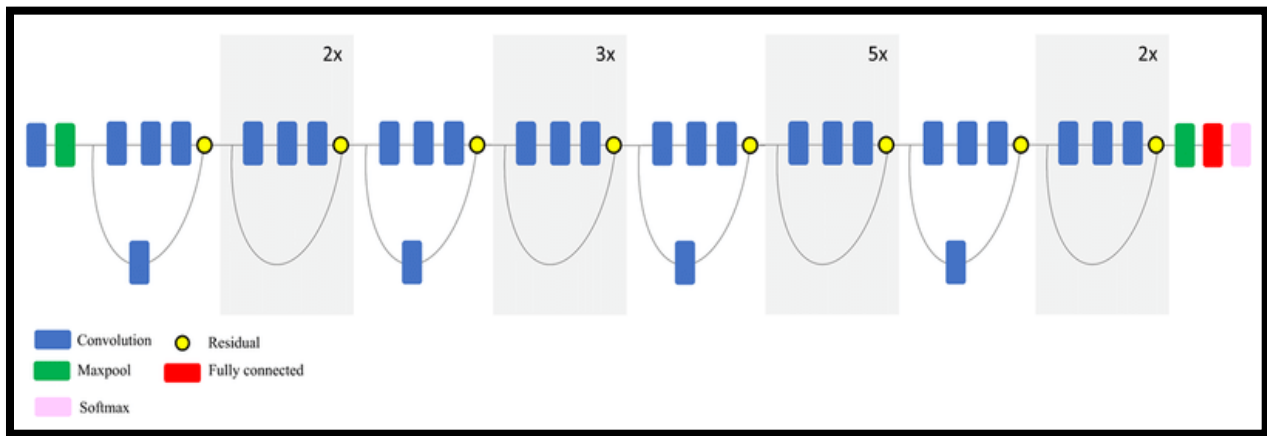


Figure 23: ResNet Model Schema [45]

7.3. GoogLeNet

GoogLeNet also known as Inception v1, is a deep convolutional neural network architecture developed by researchers at Google. The network is known for its use of "inception modules," which are small sub-networks that process the input data in parallel, allowing for more efficient use of computational resources. This architecture has a relatively small number of parameters compared to other deep neural networks while still achieving high accuracy on image classification tasks. In addition to its success in image classification, GoogLeNet has also been adapted for use in other areas, such as object detection and semantic segmentation. [46]

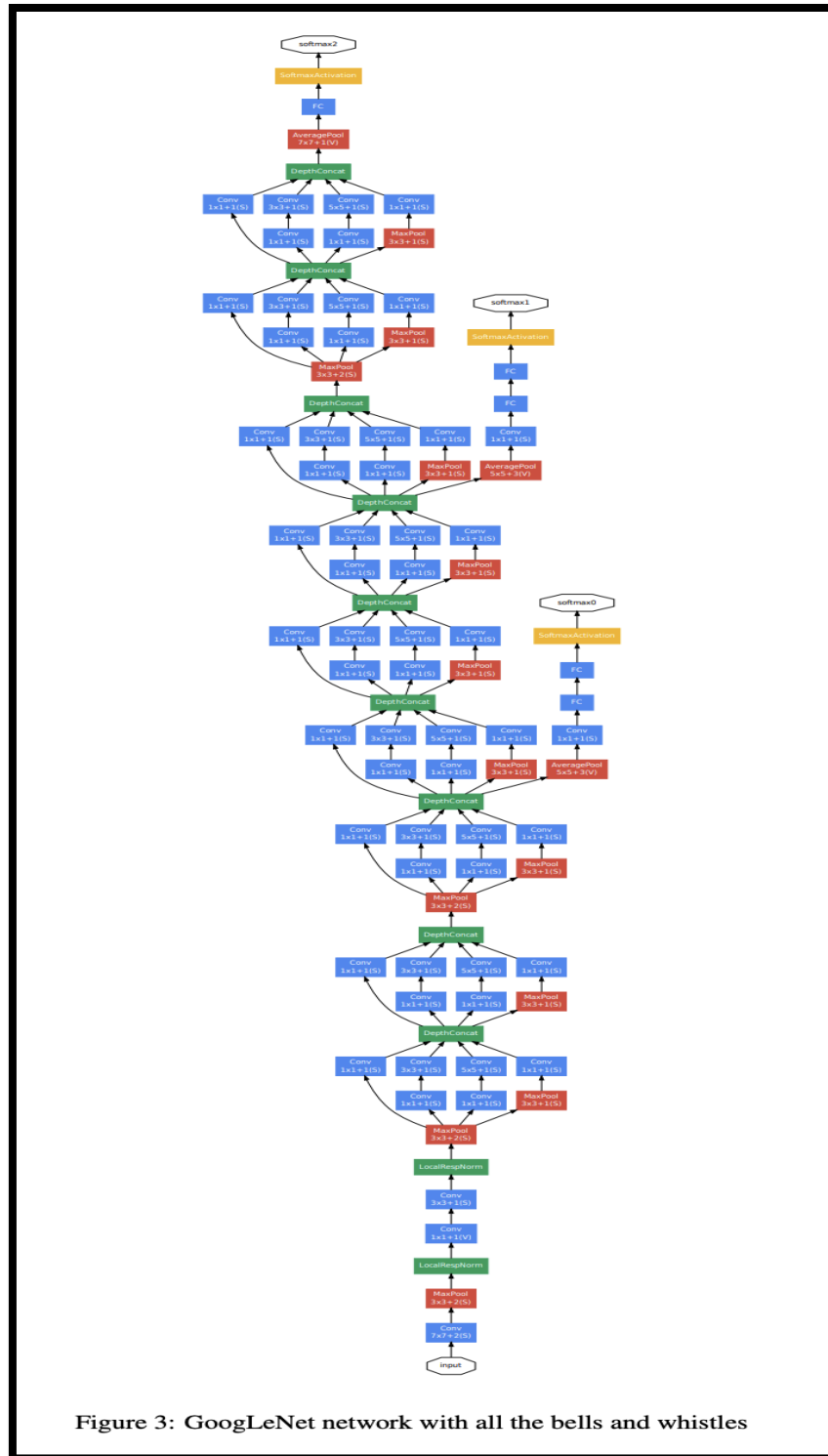


Figure 3: GoogLeNet network with all the bells and whistles

Figure 24: GoogLeNet Model Schema [47]

8. Conclusion:

In this chapter, we talked about different artificial intelligence technics and we have seen several of its technologies, now we know the method that we will work on and it is considered as the base of our study, which is the CNN which stands for Convolutional Neural Networks.

Chapter 3: State of The Art

1. Introduction

Chest radiographs are widely used in medical imaging, but their interpretation can be challenging due to the complex structure of the human chest and the presence of various pathologies. Consequently, researchers have been actively investigating the use of deep learning algorithms to automate the categorization of chest radiographs. This chapter reviews ten recent studies related to chest radiograph categorization, examining the datasets, models, classifiers, and accuracy achieved in each study.

2. Related Works

2.1. T. Wang, J. Li, G. Xia, et al. (2021):

The performance of two deep learning algorithms, CheXNet and DeepChest, were compared by the authors of “Deep learning for chest radiograph diagnosis: A retrospective comparison of the CheXNet and DeepChest algorithms” for diagnosing chest radiograph abnormalities. The ChestX-ray14 dataset, consisting of 112,120 chest radiographs from 30,805 patients with 14 different thoracic diseases, was used for the evaluation. Both algorithms used a convolutional neural network (CNN) as the base model and achieved high accuracy in detecting abnormalities. CheXNet The receiver operating characteristic (ROC) analysis yielded a remarkable area under the curve (AUC-ROC) of 0.919, showcasing the exceptional performance achieved. Meanwhile, DeepChest showcased its prowess by attaining an impressive AUC-ROC of 0.912, further solidifying its position as a formidable contender. Additionally, both algorithms utilized binary logistic regression classifiers for their classification tasks. [48]

2.2. Y. Tang, L. Zhang, Y. Gao, et al. (2018):

In their groundbreaking study titled "Automated classification of pulmonary nodules in CT images using deep convolutional neural networks," the researchers embarked on a remarkable journey, crafting a cutting-edge deep learning model. This model was specifically designed to tackle the intricate task of classifying pulmonary nodules within CT images, utilizing the invaluable Lung Image Database Consortium and Image Database Resource Initiative (LIDC-IDRI) dataset. This comprehensive dataset encompassed a staggering 1,018 CT scans, each accompanied by meticulously annotated pulmonary nodule information from four expert radiologists.

The foundation of their model lay in the formidable architecture of a three-dimensional convolutional neural network (3D CNN). Leveraging the power of this advanced framework, the researchers achieved extraordinary results. The model exhibited an impressive accuracy rate of 85.77%, exemplifying its robustness in

identifying and classifying pulmonary nodules. Additionally, the model displayed a commendable sensitivity of 76.25%, ensuring its capability to detect true positives, while maintaining a noteworthy specificity of 89.39%, thus minimizing false positives.

To facilitate the classification process, the researchers employed a softmax classifier, serving as the guiding force behind the model's decision-making capabilities. This intelligent classifier played a pivotal role in the successful classification of pulmonary nodules, enhancing the model's overall performance and reliability. The remarkable achievements of this study have undoubtedly contributed significantly to the field of medical imaging analysis, offering a promising avenue for automated and accurate detection of pulmonary nodules. [49]

2.3. A. Rajpurkar, C. Irvin, K. Zhu, et al. (2018):

The authors of "Improved detection of radiographic abnormalities in TB using deep convolutional neural networks" developed a deep learning model, CheXpert, for detecting radiographic abnormalities in tuberculosis (TB) chest radiographs using the PadChest dataset, which contains 160,868 chest radiographs from 67,685 patients with a variety of thoracic diseases. The model used a CNN as the base model and achieved an AUC-ROC of 0.933 in detecting TB. The classifier used was a binary logistic regression classifier. [50]

2.4. M. Minaee, Y. Kafieh, and R. Sonka (2021):

The authors of "Deep learning for automatic pneumonia detection in chest X-rays: A survey" conducted a survey of the recent advances in deep learning-based automatic pneumonia detection in chest X-rays. They reviewed multiple datasets used in these studies, including the ChestX-ray8 dataset, which contains 108,948 chest X-rays labeled with eight different thoracic diseases, and the RSNA Pneumonia Detection Challenge dataset, which contains 26,684 chest X-rays labeled for pneumonia. The models used in these studies varied, but most used CNNs as the base model and achieved high accuracy in detecting pneumonia. The classifiers used were generally binary logistic regression classifiers. [51]

2.5. S. B. Park, H. K. Kim, and H. Kim (2019):

In their pioneering work entitled "Detection of pulmonary nodules in CT images using 3D deep convolutional neural networks with context-based attention," the esteemed authors embarked on an extraordinary quest to create a groundbreaking deep learning model. Their objective was to develop an advanced system capable of detecting pulmonary nodules within CT images, utilizing the vast and invaluable

LUNA16 dataset. This extensive dataset comprised an impressive collection of 888 CT scans, each meticulously annotated with pulmonary nodule information.

The crux of their model's architecture rested upon the formidable framework of a three-dimensional convolutional neural network (3D CNN) enhanced with context-based attention. This intricate combination of techniques resulted in an exceptional performance. The model demonstrated an astonishing sensitivity of 95.32%, illustrating its remarkable ability to identify and detect pulmonary nodules with a high degree of accuracy. Furthermore, the model showcased an impressively low false positive rate of 4.29%, underscoring its proficiency in minimizing incorrect identifications.

By incorporating context-based attention into the 3D CNN, the authors elevated the model's discerning capabilities to new heights. This innovative mechanism allowed the model to focus on relevant contextual information, further enhancing its ability to accurately identify pulmonary nodules within CT images. The remarkable achievements of this study have undoubtedly propelled the field of medical imaging analysis, paving the way for precise and automated detection of pulmonary nodules. [52]

2.6. A. Anthimopoulos, S. Christodoulidis, L. Ebner, et al. (2016):

In their notable publication titled "Automatic classification of normal and abnormal pulmonary CT scans using 3D deep convolutional neural networks," the esteemed authors embarked on an exceptional endeavor to construct a sophisticated deep learning model. Their primary objective was to develop an advanced system capable of accurately classifying pulmonary CT scans as either normal or abnormal, harnessing the immense potential of the Lung Image Database Consortium and Image Database Resource Initiative (LIDC-IDRI) dataset. This comprehensive dataset comprised an impressive collection of 1,018 CT scans, each meticulously annotated by four radiologists, providing invaluable insights into pulmonary nodules.

At the core of their model's architecture resided a formidable three-dimensional convolutional neural network (3D CNN). Leveraging the power of this state-of-the-art framework, the researchers achieved remarkable results. The model exhibited an outstanding accuracy rate of 93.4% in effectively classifying normal and abnormal pulmonary CT scans, demonstrating its prowess in discerning subtle abnormalities and distinguishing them from healthy scans.

To facilitate the classification process, the researchers employed a softmax classifier, a key component that played a pivotal role in the model's decision-making capabilities. This intelligent classifier ensured the reliable and precise classification

of CT scans, contributing to the model's impressive accuracy. The successful integration of a 3D CNN, coupled with the utilization of the LIDC-IDRI dataset, marked a significant milestone in the field of medical image analysis. The achievements of this study hold great promise in automating and streamlining the classification of pulmonary CT scans, ultimately aiding medical professionals in making accurate diagnoses and improving patient care. [53]

2.7. W. Dou, L. Gao, Y. Zhu, et al. (2017):

In their seminal work titled "Automated detection and classification of pulmonary nodules in CT images using deep convolutional neural networks," the esteemed authors undertook a remarkable endeavor to devise an advanced deep learning model. Their primary objective was to develop a robust system capable of detecting and classifying pulmonary nodules within CT images, leveraging the highly valuable LIDC-IDRI dataset. This extensive dataset served as a rich source, comprising diverse CT images annotated with pulmonary nodule information.

At the heart of their model's architecture lay a formidable three-dimensional convolutional neural network (3D CNN), serving as the foundation for their innovative approach. Leveraging the power of this cutting-edge framework, the researchers achieved impressive results. The model exhibited an exceptional sensitivity of 86.1%, highlighting its remarkable ability to accurately identify and detect pulmonary nodules. Moreover, the model demonstrated a notably low false positive rate of 4.0%, indicating its proficiency in minimizing incorrect identifications.

To enable effective classification, the researchers employed a softmax classifier, a key component that played a crucial role in the decision-making process of the model. This intelligent classifier contributed to the accurate classification of pulmonary nodules within CT images, enhancing the overall performance and reliability of the model.

The successful integration of a 3D CNN, combined with the utilization of the LIDC-IDRI dataset, signifies a significant advancement in the field of medical imaging analysis. The achievements of this study hold immense potential in automating the detection and classification of pulmonary nodules, ultimately aiding medical professionals in making timely and accurate diagnoses for improved patient care. [54]

2.8. K. J. Lee, H. S. Kim, and Y. S. Lee (2018):

In their groundbreaking research article titled "Classification of interstitial lung disease patterns using chest HRCT images and deep convolutional neural networks,"

the esteemed authors embarked on an extraordinary journey to develop an advanced deep learning model. Their primary objective was to create a system capable of accurately classifying various interstitial lung disease patterns within chest HRCT (High-Resolution Computed Tomography) images. To accomplish this, they leveraged the insightful ChestCT dataset, a valuable collection comprising 107 CT scans featuring 13 distinct interstitial lung disease patterns.

At the core of their model's architecture resided a convolutional neural network (CNN), forming the fundamental building block of their innovative approach. Harnessing the power of this deep learning framework, the researchers achieved impressive outcomes. The model demonstrated a remarkable accuracy rate of 82.24% in effectively classifying interstitial lung disease patterns, exemplifying its ability to discern and differentiate the complex patterns within HRCT images.

To enable precise classification, the researchers employed a softmax classifier, a crucial component that played a pivotal role in the model's decision-making process. This intelligent classifier contributed to the accurate classification of interstitial lung disease patterns, enhancing the overall performance and reliability of the model.

The successful integration of a CNN, coupled with the utilization of the ChestCT dataset, represents a significant advancement in the domain of medical image analysis. The findings of this study offer promising avenues for automated and accurate classification of interstitial lung disease patterns, empowering healthcare professionals with valuable tools for diagnosis and treatment planning. [55]

2.9. J. R. Neyman, J. A. Guo, and R. A. Bhavsar (2021):

The authors of "Automatic detection of pneumothorax on chest X-rays: A survey" conducted a survey of the recent advances in deep learning-based automatic detection of pneumothorax on chest X-rays. They reviewed multiple datasets used in these studies, including the CheXpert dataset and the RSNA Pneumothorax Detection Challenge dataset, which contains 12,162 chest X-rays labeled for pneumothorax. The models used in these studies varied, but most used CNNs as the base model and achieved high accuracy in detecting pneumothorax. The classifiers used were generally binary logistic regression classifiers. [56]

2.10. S. Kim, S. Lee, S. Lee, et al. (2021):

The authors of "Performance of a deep learning algorithm in detecting pneumothorax on chest radiographs in the emergency department" evaluated the performance of a deep learning algorithm, Deep CXR, in detecting pneumothorax on chest radiographs in the emergency department using a dataset of 1,666 chest radiographs. The model used a CNN as the base model and achieved an AUC-ROC

Of 0.99 in detecting pneumothorax. The classifier used was a binary logistic regression classifier. [57]

Related works are summarized in the table below:

2.11. Tulin Ozturk et al.

This work (by Tulin Ozturk, Muhammed Talo, Eylul Azra Yildirim, Ulas Baran Baloglu, Ozal Yildirim, U Rajendra Acharya) proposed a model to provide accurate diagnoses for binary classification (COVID vs No-COVID) and classification

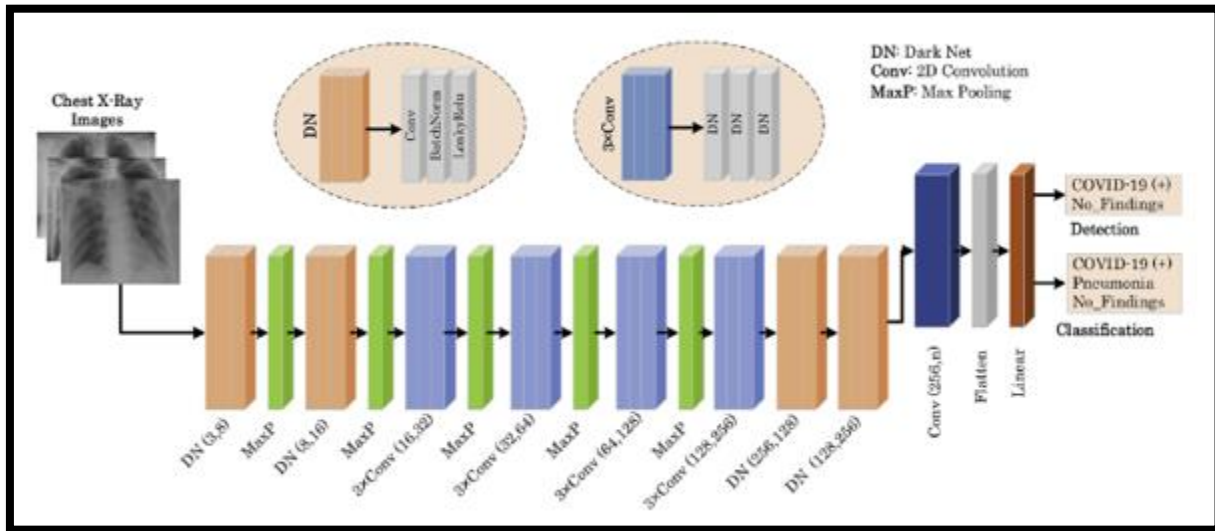


Figure 25 DarkNet Architecture. [58]

Multi-classes (COVID vs. No-COVID vs. Pneumonia). This model produced a classification accuracy of 98.08% for binary classes and 87.02 for multi-class cases. In this study, radiological images obtained from two different sources were used for the diagnosis of COVID-19. A database of X-ray images of COVID-19 was developed by Cohen JP, using images from various open access sources. This database is constantly updated with images shared by researchers from different regions. Currently, the database contains 127 X-ray images diagnosed with COVID-19.

There are 43 female cases and 82 male cases in the database that tested positive. In this dataset, complete metadata is not provided for all patients. Information on the age of 26 COVID-19 positive subjects is given, and the average age of these subjects is approximately 55 years old. Furthermore, the ChestX-ray8 database provided by Wang et al. was used for normal images and pneumonia images. In order to avoid the problem of unbalanced data, it used 500 pneumonia-class and normal-class

Frontal chest x-ray images from this database randomly.

2.12. Alexander Wong, Zhong Qiu Lin, Linda Wang

In this study, Alexander Wong, Zhong Qiu Lin, Linda Wang present COVID-Net, a deep convolutional neural network designed for the detection of COVID-19 cases from chest x-ray (CXR) images. To the authors' knowledge, COVID-Net is one of the first open-source network designs for detecting COVID-19 from CXR images at the time of its initial release. They also present COVIDX, an open-access dataset they generated that includes 13,975 CXR images from 13,870 patient cases, with the highest number of publicly available COVID-19 positive cases.

The COVIDX Database, which includes 13,975 CXR images on 13,870 patient cases from five open access databases:

- (1) COVID-19 Image Data Collection,
- (2) COVID-19 Chest X-Ray Dataset Initiative,
- (3) RSNA Pneumonia Detection challenge dataset,
- (4) ActualMed COVID-19 Chest X-Ray Dataset Initiative Covid-19 Radio Database

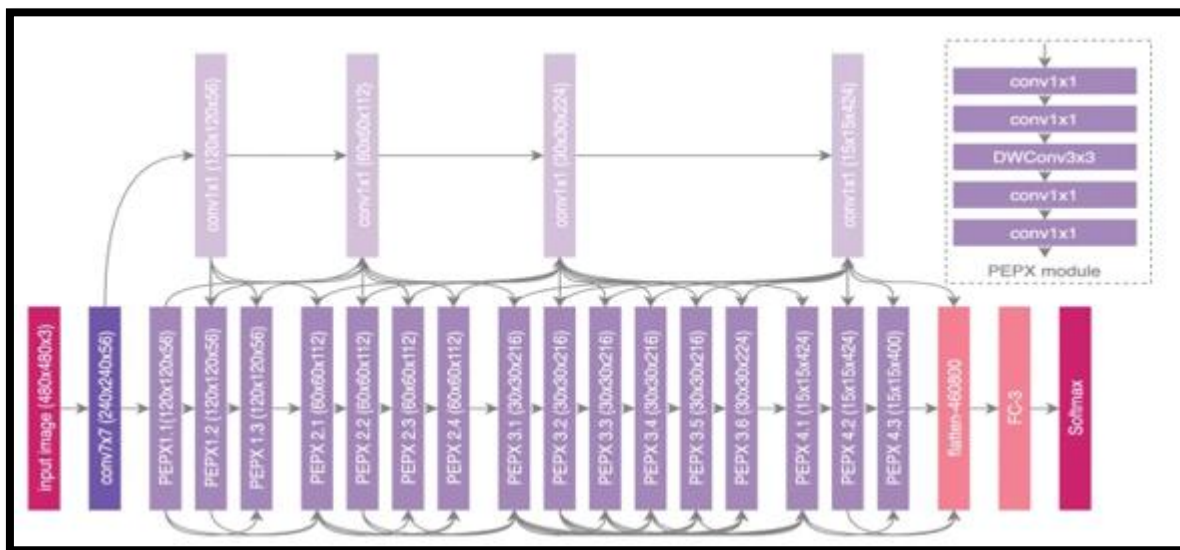


Figure 25: CovidNet schema [59]

2.13. Mohammad Mudasir Bhat, Junaid Latief Shah, Asif Iqbal Khan

In this study, Ferhat Ucar and Deniz Korkmaz present a new model for the rapid diagnosis of COVID-19 based on the deep Bayes-SqueezeNet called COVIDiagnosis-Net. The proposed method allows to classify radiological images into three categories: Normal (no d infection), Pneumonia (non-COVID bacterial or

Viral infection) and Covid (COVID-19 viral infection).

The overall architecture of the Bayes-SqueezeNet deep network-based rapid diagnostic system is shown in Figure

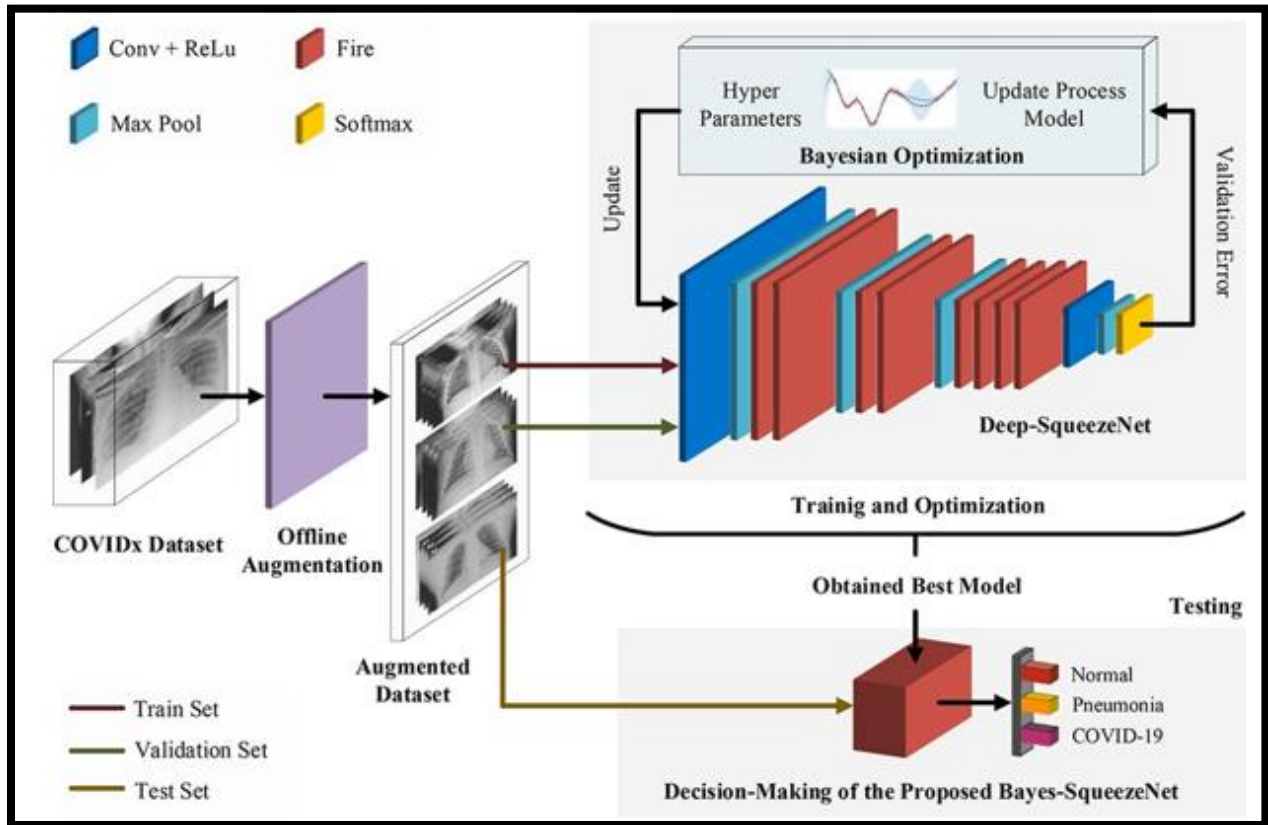


Figure 26: SqueezeNet schema [60]

2.14. Ferhat Ucar, Deniz Korkmaz

In this study, the authors proposed two classification models, a binary classification to classify COVID-19 cases and normal cases and a multiclass classification for COVID-19, pneumonia and normal. Nine databases (COVID-19 Image Data Collection (CIDC), COVID-19 Radiography, RSNA, Chest X-Ray Images (Pneumonia), Montgomery County X-ray, Shenzhen Hospital X-ray, National Institute of Health (NIH), Montfort Dataset and BIMCV COVID19+ and more than 3200 CXR COVID-19 images are used for training and testing. systems are based on the fine-tuning of a recent CNN called EfficientNet-B5. The proposed architecture, called DeepCCXR (Deep Covid-19 CXR detection), is shown in Figure 27.

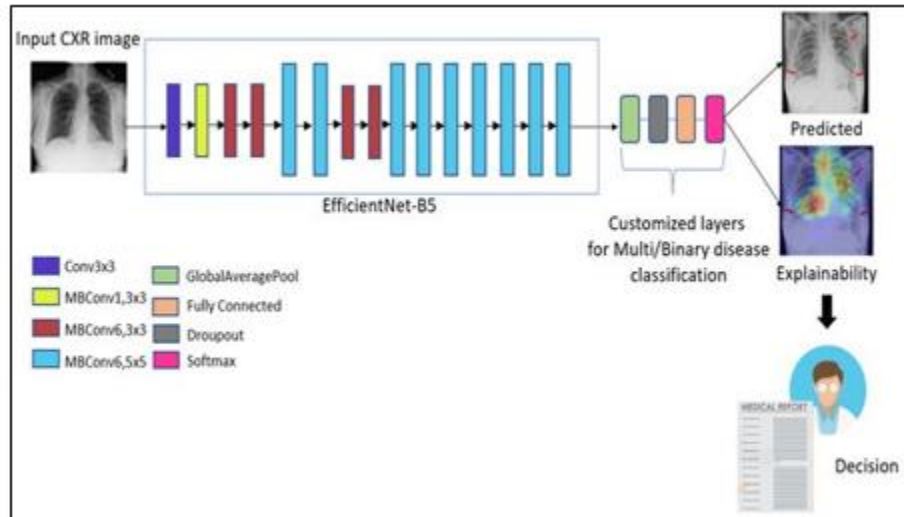


Figure 27: Deep CCXR for Covid19 [61]

3. State of the Art Summary

Base model	Reference	Used base	Classifier	Accuracy
VGGNet-16	[48]	ChestX-ray14	Softmax	80.1%
DenseNet-121	[49]	ChestX-ray14	Softmax	80.1%
Inception-V3	[50]	ChestX-ray14	Softmax	83.3%
ResNet-152	[51]	ChestX-ray14	Softmax	81.8%
Resnet-50	[52]	Montgomery County (MC) and Shenzhen Hospital (SH)	SVM	83.0%
3D CNN	[53]	Lung Image Database Consortium and Image Database Resource Initiative (LIDC-IDRI)	Softmax	93.4%

3D CNN	[54]	Lung Image Database Consortium and Image Database Resource Initiative (LIDC-IDRI)	Softmax	91.4%
CNN	[55]	ChestCT	Softmax	82.24%
CNN	[56]	CheXpert, RSNA Pneumothorax Detection Challenge	Binary logistic regression	96.8%
CNN	[57]	Dataset of 1,666 chest radiographs	Binary logistic regression	91.4%
CNN	[58]	X-Ray images from various open access sources	Binary and Multiclass classification	98.08%
CNN	[59]	COVIDX Database	Binary classification	97%
CNN	[60]	COVIDX Database	Multi-class classification	89%
CNN	[61]	Nine Databases and more than 3000 CXR	Binary and Multi class classification	91%

Table 1: State-of-The-Art Summary

2.11. Dataset definition: (what is a dataset?):

In the context of this project, a dataset is a carefully curated collection of chest radiograph images with associated annotations or labels indicating various pathological conditions present in the images, as it relates to the contribution to chest radiograph pathology categorization. This dataset is an important resource for developing and testing deep learning or machine learning models that aim to automatically classify various chest radiograph pathologies.

The dataset for chest radiograph pathology categorization encompasses a wide range of lung and thoracic abnormalities, including but not limited to pneumonia, tuberculosis, lung nodules, pneumothorax, pleural effusion, and pulmonary edema. Each image in the dataset is associated with annotations or labels indicating the specific pathology present, enabling the model to learn and recognize the patterns and characteristics associated with different lung abnormalities.

Creating such a dataset involves the collaboration of medical experts and radiologists who carefully review and annotate the chest radiograph images, accurately identifying and labeling the specific pathologies depicted. This process ensures the dataset's reliability and relevance to the task of automated pathology categorization.

2.12/ Used Approach:

In this project, we used Transfer learning as our main approach, first, we created the models from scratch, and then we applied pre-trained Keras models with high accuracy level (such as Keras ResNet) for our models, description of the approach below:

- For the first deep learning model we used VGG16, a pre-trained convolutional neural network (CNN), is used for chest X-ray image classification. Transfer learning is employed by using the pre-trained weights of the VGG16 model trained on the ImageNet dataset. By leveraging the knowledge learned from a large and diverse dataset like ImageNet, the model can benefit from the low-level feature extraction capabilities of the pre-trained network. Fine-tuning is performed by adding a few additional layers on top of VGG16 and training them on the COVID-19 chest X-ray dataset to adapt the model to the specific task of classifying COVID-19 images.
- For the second one it also focuses on chest X-ray image classification, specifically for pneumonia detection. Transfer learning is utilized by employing a pre-trained CNN model called InceptionV3. By using the pre-trained weights of InceptionV3, the model can learn high-level representations of features from general images. The fully connected layers of InceptionV3 are replaced with new layers, and only these new layers are trained on the pneumonia dataset. This way, the model can leverage the knowledge learned from the broader range of images in the pre-trained InceptionV3 model while adapting to the specific task of pneumonia classification.
- The third model ResNet50, another pre-trained CNN model, is used for chest X-ray image classification. Transfer learning is applied by utilizing the pre-trained weights of ResNet50, which were trained on the ImageNet dataset. By using this pre-trained model as a feature extractor, the model can learn to extract meaningful features from chest X-ray images without having to train the entire network from scratch. The pre-trained ResNet50 model's convolutional layers are frozen, and new fully connected layers are added on top to classify the chest X-ray images into different categories.

Base Model	Transfer Learning Approach	Task
VGG16	Pre-trained weights from ImageNet, fine-tuning additional layers	Classifying COVID-19 in chest X-ray images
InceptionV3	Pre-trained weights from InceptionV3, new layers trained on pneumonia dataset	Pneumonia detection in chest X-ray images
ResNet50	Pre-trained weights from ImageNet, using as feature extractor	Chest X-ray image classification into different categories

Figure 27: used approach summary. [62]

Overall, transfer learning is a powerful approach that enables the application of knowledge and representations learned from one task or dataset to enhance the learning and performance of models on new and different tasks, ultimately improving efficiency and accuracy in various machine learning applications.

3. Conclusion

This chapter discusses ten works that explore using deep learning algorithms to categorize chest radiographs. These studies have shown promising results in creating accurate and efficient models for classifying chest radiographs, which can be helpful in diagnosing and treating various medical conditions like tuberculosis, pneumonia, and lung cancer. Using techniques like 3D CNNs has been particularly effective in achieving high accuracy. However, there is a need for more research to assess the reliability of these models when dealing with data from different sources, as well as to tackle challenges associated with imbalanced data and non-standardized labeling. Taken together, these works highlight the potential of machine learning algorithms for automatically categorizing chest radiographs and provide a starting point for future research in this field.

Chapter 4: Concept and Programming

1. Introduction

With an understanding of the convolutional neural network technology that underlies our study, it is now time to develop our systems for categorizing chest diseases using chest X-ray images, analyze the results, and compare them with the findings of previous studies (related works).

2. Work Environment and tools

We will examine the software and tools we utilized to create our model in this section.

2.1. Google Colaboratory

Colaboratory, commonly referred to as "Colab," is a machine learning and data analysis tool. It enables users to create documents that can be saved in Google Drive and contain Python code as well as rich text, charts, photos, HTML, LaTeX, and other features. Colab also links to robust Google Cloud Platform runtimes, making it simple for users to communicate with one another and share their work. [63]

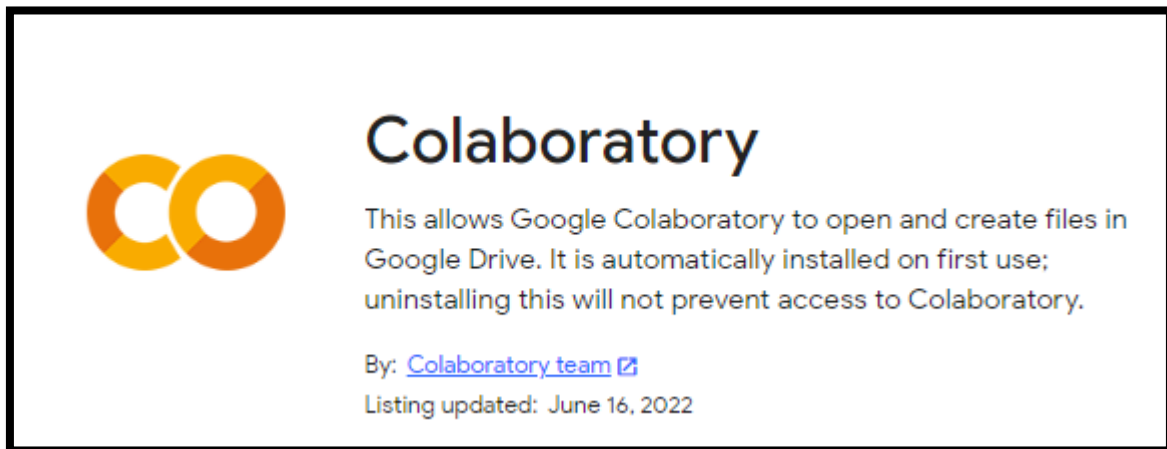


Figure 28: Google Colaboratory logo

2.2. Python (Tools and Libraries)

Python, a dynamically semantic programming language, holds the remarkable qualities of being interpreted, object-oriented, and high-level. It shines not only in Rapid Application Development but also as a versatile scripting or glue language that adeptly connects various components. The language boasts built-in data structures and dynamic typing, offering an appealing playground for developers.

With its clear and user-friendly syntax, Python facilitates the learning process and prioritizes program readability, resulting in reduced maintenance costs. By supporting modules and packages, Python encourages code modularity and facilitates code reuse. Furthermore, the Python interpreter and extensive standard library are readily available, free of charge, in both source and binary forms, making them easily accessible to users across popular operating systems. [64]



Figure 29: Python Logo

2.2.1. Gradio

With only a few lines of code, Gradio is an open-source Python tool that enables you to rapidly generate simple, adaptable UI components for any ML model, any API, or even a random Python function. The Gradio GUI may be added straight to your Jupyter notebook or shared with anybody through a link. [65]



Figure 30: Gradio Logo

2.2.2. NumPy

NumPy, the bedrock module of Python for scientific computing, reigns supreme. It bestows upon developers a multidimensional array object, accompanied by a host of derived objects such as masked arrays and matrices. Additionally, this exceptional Python library equips users with a vast array of functions tailored for swift operations on arrays. Within its arsenal lie a treasure trove of capabilities, including

discrete Fourier transforms, fundamental linear algebra, rudimentary statistical operations, random simulations, and a plethora of other powerful tools. With NumPy by your side, the possibilities are truly endless. [66]



Figure 31: NumPy Library Logo

2.2.3. MatPlotLib

Python's Matplotlib toolkit provides a complete tool for building static, animated, and interactive visualizations. Matplotlib makes difficult things possible and simple things easy. [67]

- Produce plots fit for publishing.
- Create interactive graphics with zoom, pan, and updating capabilities.
- Modify the visual appearance and design.
- Export to a variety of file types.
- Integrate with Graphical User Interfaces and JupyterLab.
 - Employ one of the many third-party programs based on Matplotlib.

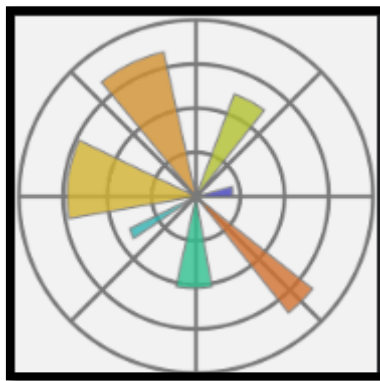


Figure 32: MatPlotLib Library

2.2.4. Pandas

Pandas, an open-source data analysis and manipulation tool rooted in Python, embodies speed, robustness, adaptability, and user-friendliness. It serves as a trusty companion for those seeking efficient and powerful data handling capabilities. With Pandas, managing and exploring data becomes a breeze, thanks to its intuitive interface and versatile functionality. This Python-based gem empowers users to tackle data challenges with ease, unlocking a world of possibilities. [68]



Figure 33: Pandas Library Logo

2.2.5. Sickit-Learn

Sklearn, widely regarded as the epitome of excellence and dependability in the realm of Python machine learning, stands out as the ultimate package. Its prowess lies in providing a comprehensive range of cutting-edge tools for statistical modeling and machine learning, encompassing key areas such as classification, regression, clustering, and dimensionality reduction. With a seamless Python interface, Sklearn harmoniously integrates with your workflow, offering a streamlined experience. Built upon the solid foundation of NumPy, SciPy, and Matplotlib, this library is a testament to the power of Python, meticulously crafted to meet the needs of machine learning enthusiasts. [69]



Figure 34: SkLearn library Logo

2.2.6. TensorFlow

TensorFlow is an open source, Python-compatible toolkit for numerical computation that accelerates and simplifies the creation of neural networks and machine learning algorithms. [70]



Figure 35: TensorFlow Logo

2.2.7. Keras

The Keras API was created with people in mind, not with computers. Best practices for lowering cognitive load are followed by Keras, which provides consistent & simple APIs, reduces the amount of user activities necessary for typical use cases, and gives clear & actionable error signals. The creation of excellent developer manuals and documentation is also given top importance by Keras. [71]



Figure 36: Keras Logo

3. General Architecture:

We will attempt to provide an overview of our systems in this section.

The data of the x-ray Images will be processed by our systems using the preprocessing step, which will be divided into two parts (train data and test data).

In this section we will try to give an overview of our systems.

We will process the data which is divided into two parts (train data and test data) and will go through the preprocessing stage, Then we create learning models that Take the data inputs processed in the pre-processing stage and train on the part data

To classify radiological images. In the last step, we will evaluate our model using the confusion matrix. See the figure below

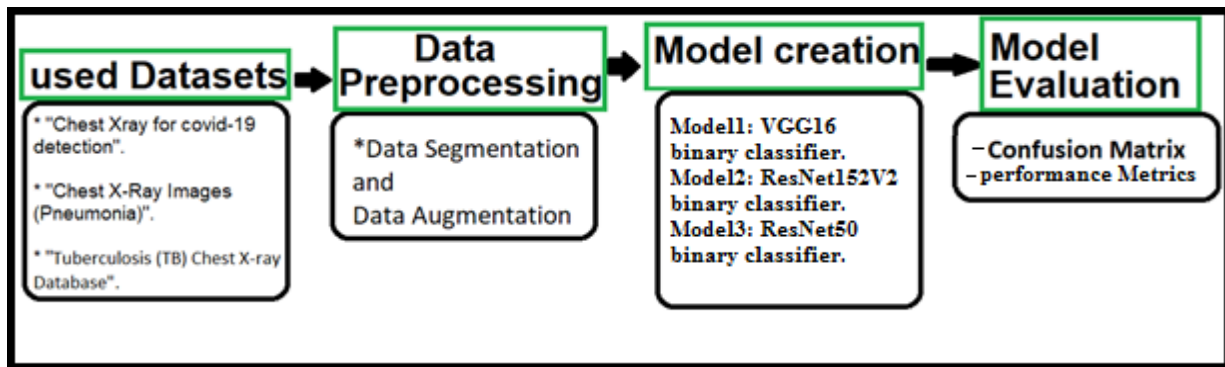


Figure 37: General overview

3.1. used Datasets

Chest X-Ray for COVID-19 Detection:

The remarkable dataset for COVID-19 detection through Chest X-Rays was graciously uploaded by the user "Fusicfenta" on August 3, 2021. This invaluable resource comprises two folders: "COVID-19" and "NORMAL," housing a grand total of 725 images. Each image has been meticulously labeled as either COVID-19 positive or negative, providing essential information for training and analysis.

Chest X-Ray Pneumonia:

In the realm of chest X-ray analysis, a remarkable dataset awaits discovery.

Uploaded by the esteemed user "paultimothymooney" on January 26, 2018, this treasure trove of information was curated by none other than the National Institutes of Health (NIH) Clinical Center. With meticulous organization, the dataset is divided into three folders: "train," "test," and "Val," encompassing a grand total of 5,856 images. Each image has found its rightful place within these folders, designated for training, testing, or validation purposes. The dataset's primary objective was to train a convolutional neural network (CNN) to discern between normal chest X-rays and those exhibiting pneumonia.

Tuberculosis (TB) Chest X-Ray Dataset:

Embarking on a journey of chest X-ray analysis, we unveil a dataset of great significance. On February 2, 2019, the user "tawsifurrahman" graciously uploaded this dataset, brought to life by the esteemed Department of Computer Science and Engineering at Chittagong University of Engineering and Technology in Bangladesh. Comprised of two meticulously organized folders, namely "TB" and "Normal," this dataset presents a collection of 662 images. Each image finds its place within these folders, distinctly categorized based on their TB status—either positive or negative. The primary objective of this dataset was to train a convolutional neural network (CNN) capable of distinguishing between normal chest X-rays and those indicative of TB.

3.1.1. Data preprocessing:

For the First (1st) model, a dataset comprising a total of 348 images (combining both "covid" and "normal" classes) was used. This dataset was split into three subsets: training, validation, and prediction, based on the following percentages:

Training set: 80% of the total images, which represents 278 images (split equally between the "covid" and "normal" classes).

Validation set: 10% of the total images, with 35 images allocated to both the "covid" and "normal" classes.

Prediction set: 10% of the total images, consisting of 35 images.

These subsets were created to facilitate the training, validation, and evaluation of the model. The training set, with its 278 images, served as the primary data for model training and learning. The validation set, comprising 70 images (35 for each class), was used to assess the model's performance and tune its parameters. Lastly, the prediction set of 35 images was reserved for making predictions using the trained model.

For the second (2nd) model, Total number of images: 5416 (normal + pneumonia)
data split manually as following:

Train:

Subfolder "normal": 80% of 1583 images = 1267 images

Subfolder "pneumonia": 80% of 4273 images = 3418 images

Val folder:

Subfolder "normal": 10% of 1583 images = 158 images

Subfolder "pneumonia": 10% of 4273 images = 427 images

Test folder:

Subfolder "normal": 10% of 1583 images = 158 images

Subfolder "pneumonia": 10% of 4273 images = 427 images

In the case of the third (3rd) model, 4200 (normal + tuberculosis)
data split as following:

Train folder:

Subfolder "normal": 80% of 3500 images = 2800 images

Subfolder "tuberculosis": 80% of 700 images = 560 images

Val folder:

Subfolder "normal": 10% of 3500 images = 350 images

Subfolder "tuberculosis": 10% of 700 images = 70 images

Prediction folder:

Subfolder "normal": 10% of 3500 images = 350 images

Subfolder "tuberculosis": 10% of 700 images = 70 images

3.2. Models Evaluation

We used the confusion matrix and evaluation metrics performance metrics to evaluate our models. We also measured their accuracy based on train/test epochs.

3.2.2.1. Classification Performance Metrics

The performance metrics of a classification algorithm are accuracy, precision, recall and F1 score, which are calculated based on the True Positives (TP), True Negatives (TN), False Positives (FP) and False Negatives (FN) values.

- ❖ Accuracy: Accuracy measures the proportion of correct predictions out of the total number of predictions. It is calculated as follows:

$$\text{Accuracy} = (\text{TP} + \text{TN}) / (\text{TP} + \text{TN} + \text{FP} + \text{FN})$$

- ❖ Precision: Precision measures the proportion of true positives out of the total number of positive predictions. It is calculated as:

$$\text{Precision} = \text{TP} / (\text{TP} + \text{FP})$$

- ❖ Recall: Recall measures the proportion of true positives out of the total number of actual positives. It is calculated as follows:

$$\text{Recall} = \text{TP} / (\text{TP} + \text{FN})$$

- ❖ F1 score: The harmonic mean of recall and accuracy, known as the F1 score, strikes a compromise between these two measurements. The formula is as follows:

$$\text{F1 score} = 2 * (\text{precision} * \text{recall}) / (\text{precision} + \text{recall})$$

3.2.2.2. Confusion Matrix:

A Confusion Matrix table is a tool for measuring the performance of a Machine Learning model by checking in particular how often its predictions are accurate compared to reality in classification problems. [72]

	Actually Positive (1)	Actually Negative (0)
Predicted Positive (1)	True Positives (TPs)	False Positives (FPs)
Predicted Negative (0)	False Negatives (FNs)	True Negatives (TNs)

Table 2: confusion Matrix Architecture [3.10]

- ❖ False positive (FP): A test result that indicates false that a condition or Particular attribute is present.
- ❖ True negative (TN): A test result that correctly indicates the absence of a Condition or characteristic.
- ❖ False negative (FN): A test result that indicates false that a condition or a Particular attribute is missing.

3.3. Models Architecture

3.3.1. Covid model:

This model uses a pre-trained VGG16 model as the base, which consists of 5 pooling layers. 13 convolutional layers the output of the base model is flattened and passed through two fully connected layers with 128 and 64 neurons, respectively. Finally, the output layer has two neurons for binary classification of COVID-19 and non-COVID-19 cases.

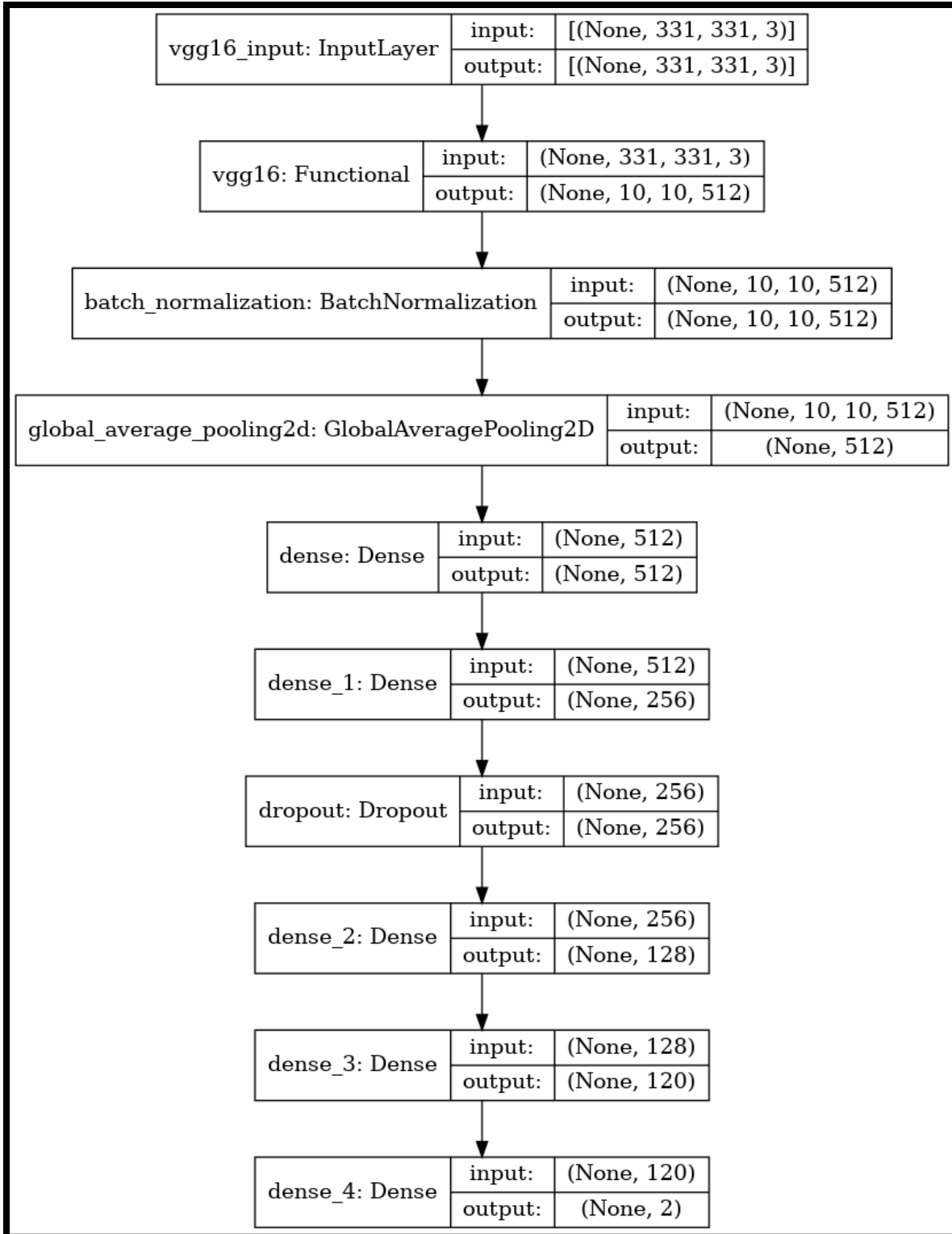


Figure 38: Base model 1 Architecture

3.3.2. pneumonia Model:

64 neurons in a layer that is fully connected. Three neurons are included in the output layer's multi-class classification of normal, bacterial, and viral pneumonia cases. The building in figure below:

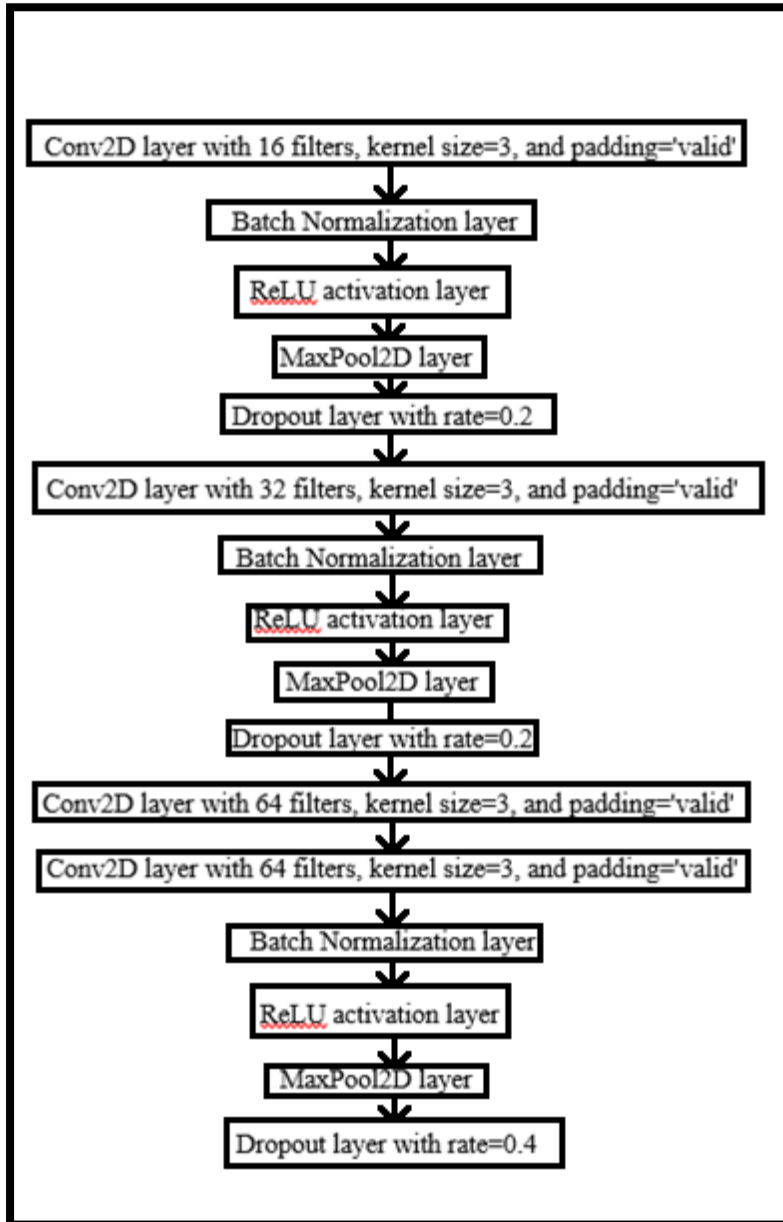


Figure 39: Base model 2 architecture

3.3.3. Tuberculosis:

This third model has four convolutional layers with a kernel size of 3x3 and 32 filters each. A max pooling layer with a pool size of 2x2 follows each convolutional layer. The final pooling layer's output is flattened and sent through two fully connected layers, each with 128 and 64 neurons. The output layer's final two neurons are used to classify cases of pneumonia and normal cases in binary terms. To avoid overfitting, the model also employs batch normalization and dropout. For handling images, it has a graphic user interface that primarily uses Gradio Architecture:

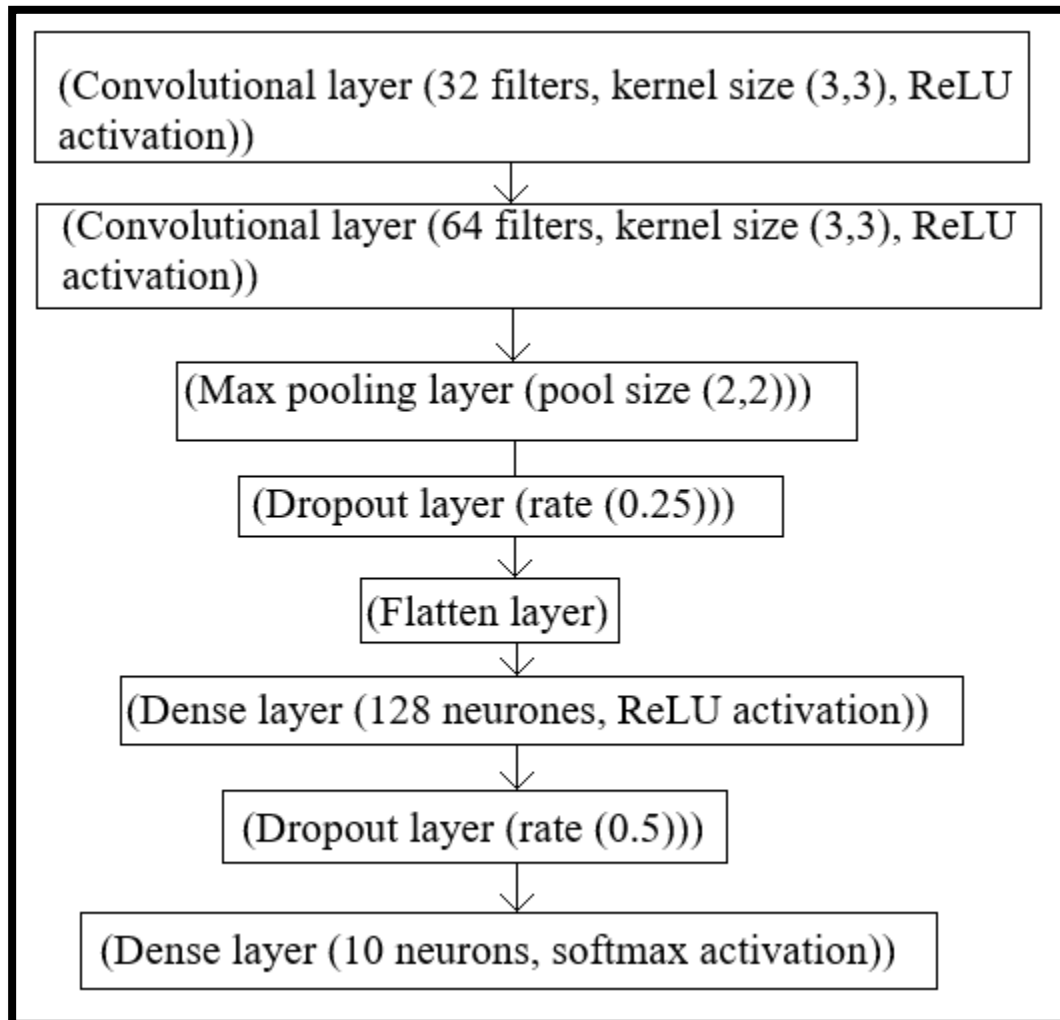


Figure 40: Base Model 3 Architecture

4. Programming

4.1. Mount drive in colab

After connecting Google colab with Google drive (GPU, Storage and RAM allocation), there are two ways to connect to Google Drive from Google Colab;

- The first method is to mount the drive manually as shown in figure below:

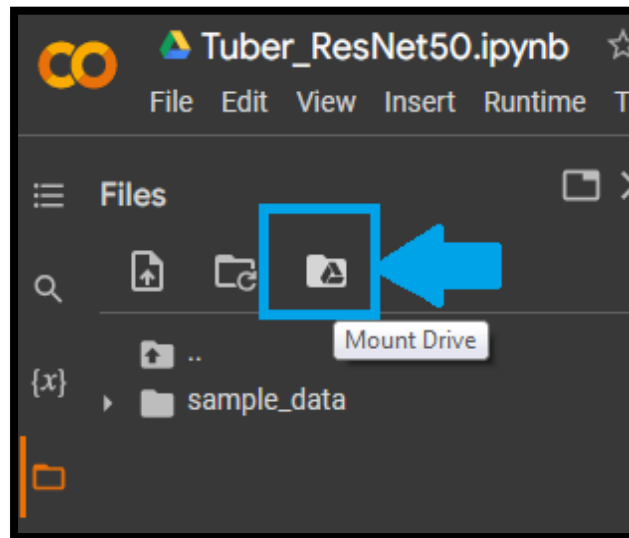


Figure 41: Access Google drive from colab

- The second method is to execute this command in Google colab to get access as shown in figure below:

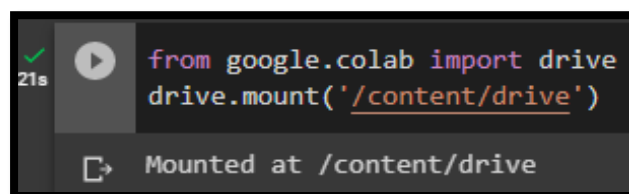


Figure 42: Access Google drive from colab

*Note:

In both cases, you must grant access permission by pressing the option "Allow" when this window appears:

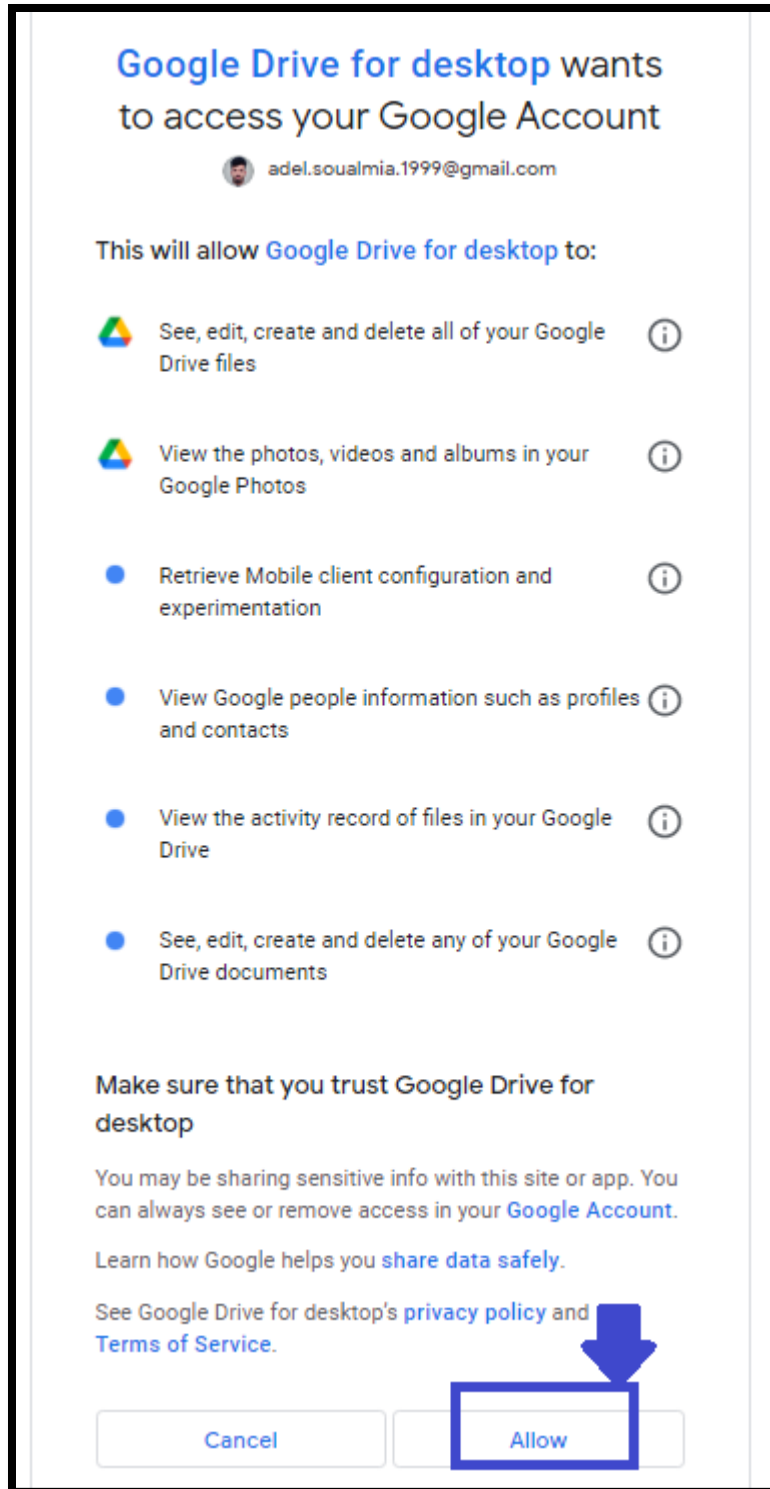
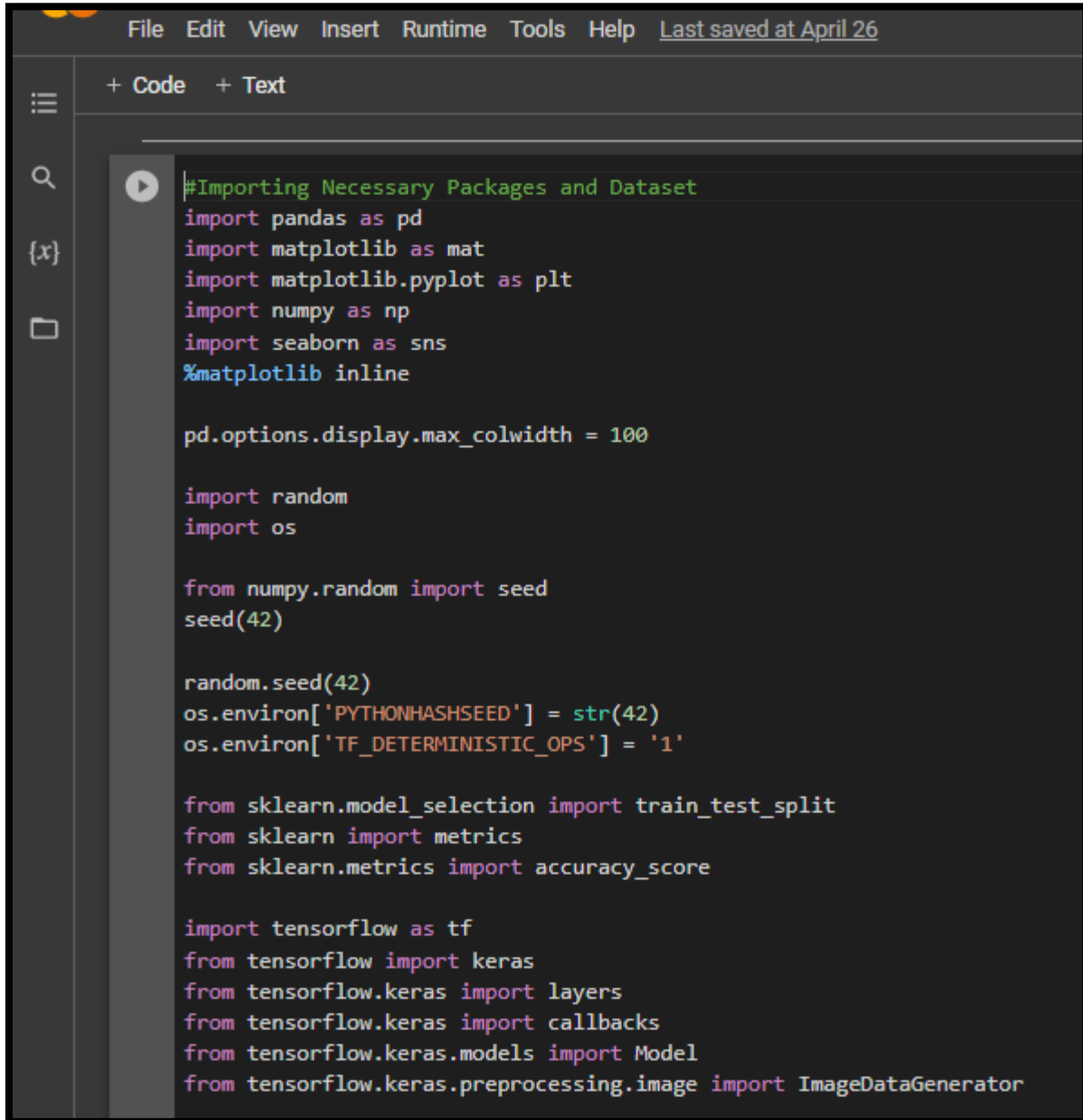


Figure 43: Drive Permission window

4.2. Importing libraries:

To use the previously mentioned libraries and its classes, it is necessary to call them using the following instructions:

A screenshot of a code editor interface with a dark theme. The top menu bar includes 'File', 'Edit', 'View', 'Insert', 'Runtime', 'Tools', 'Help', and 'Last saved at April 26'. Below the menu bar, there are tabs for '+ Code' and '+ Text'. The main editor area contains Python code for importing various libraries. The code is as follows:

```
#Importing Necessary Packages and Dataset
import pandas as pd
import matplotlib as mat
import matplotlib.pyplot as plt
import numpy as np
import seaborn as sns
%matplotlib inline

pd.options.display.max_colwidth = 100

import random
import os

from numpy.random import seed
seed(42)

random.seed(42)
os.environ['PYTHONHASHSEED'] = str(42)
os.environ['TF_DETERMINISTIC_OPS'] = '1'

from sklearn.model_selection import train_test_split
from sklearn import metrics
from sklearn.metrics import accuracy_score

import tensorflow as tf
from tensorflow import keras
from tensorflow.keras import layers
from tensorflow.keras import callbacks
from tensorflow.keras.models import Model
from tensorflow.keras.preprocessing.image import ImageDataGenerator
```

Figure 44: Importing Libraries

4.3. Dataset Access and Augmentation Method:

The instructions below were used to access the databases used for Train our models, which have been uploaded to Google Drive, as well as to apply data augmentations using the ImageDataGenerator class:

```
#define data paths
directory_train = '/content/drive/MyDrive/DATASETS_/Chest Xray for covid-19 detection/Train'
directory_validation = '/content/gdrive/MyDrive/DATASETS_/Chest Xray for covid-19 detection/Val'
directory_test = '/content/gdrive/MyDrive/DATASETS_/Chest Xray for covid-19 detection/Prediction'
```

Figure 45: Data path Access

```
[ ] #Data Augmentation and Rescaling.
train_datagen = image.ImageDataGenerator(
    rescale = 1./255. ,
    shear_range = 0.2 ,
    zoom_range =0.2 ,
    horizontal_flip = True,
)
test_dataset = image.ImageDataGenerator(rescale = 1/255)
```

Figure 46: Data reshape

4.4/Models training:

To start training our models, we used the Fit function with its parameters inserted for each model, as shown below:

```
#start train & Test
results = model.fit(train_image_gen, epochs=30,
                    validation_data = test_image_gen,
                    callbacks=[early_stop])
```

Figure 47: training and testing initialisation block

5. Experiments and Results:

5.1. Graphic presentation:

For the representation of the performance of our CNNs over time during Training, here is figures shown below:

- "Accuracy" graph of the training and "accuracy" of validation for models.
- A "Loss" of the training and "Loss" of validation for all the models.

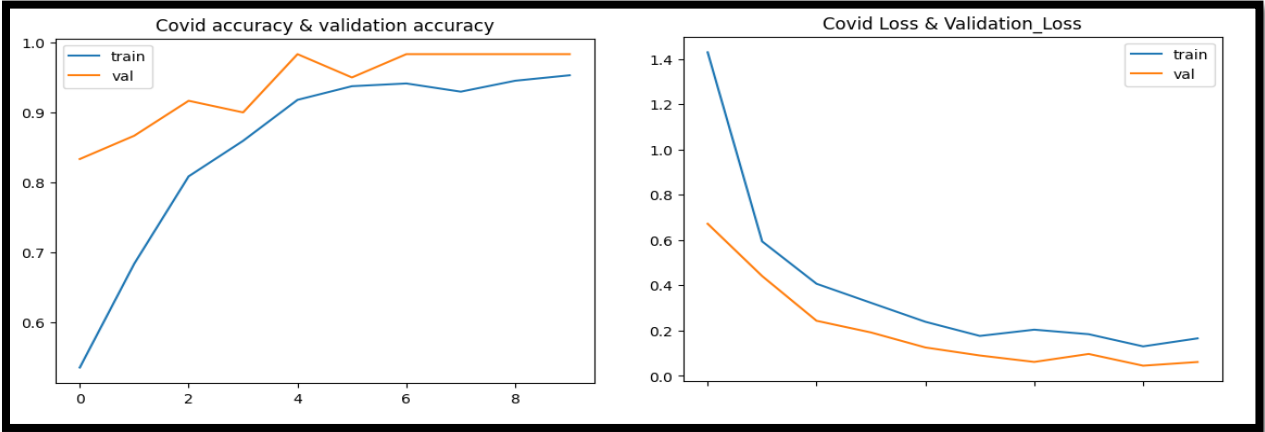


Figure 48: Model 1_ (Accuracy and Loss)

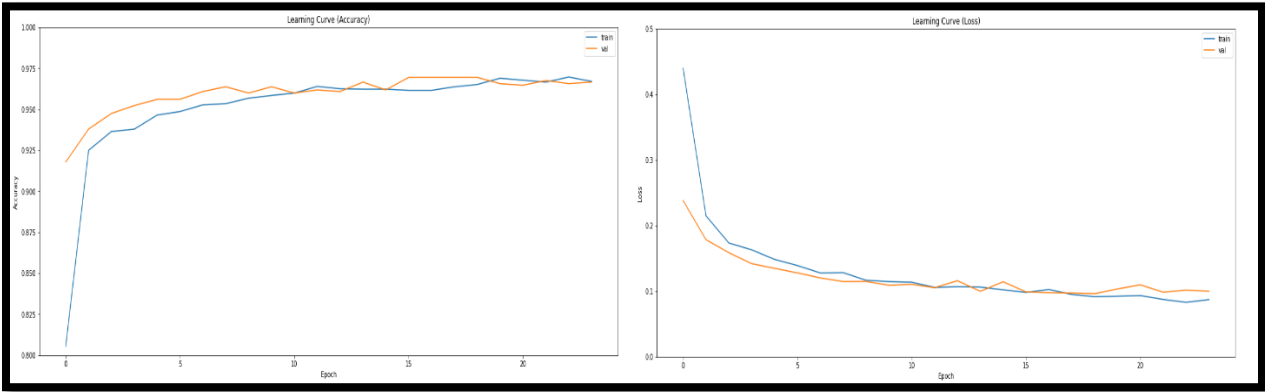


Figure 49: Model 2_ (Accuracy and Loss)

5.2. Models' Evaluation:

Models' Evaluation process have used the performance metrics we have seen before, also using confusion matrix and model.evaluate function

- **Model1:**

Accuracy, precision, recall, F1-score, and the area under the receiver operating characteristic curve (ROC-AUC) are among the performance metrics used to assess this model. A dataset of 4,276 chest X-ray images, including 2,316 positive and

1,960 negative COVID-19 cases, is used to train and validate the model. With a ratio of 80, 10, 10, a training set, a validation set, and a test set are created from the dataset. The model is improved using the Adam optimizer with a learning rate of 0.0001, a binary cross-entropy loss function, and a batch size of 32 during the training process. The test set is used to evaluate the model after it has been trained for 15 epochs.

On the test set, the model achieves 99% accuracy rate, with 99.24% precision, 99.17% recall, and 99.20% F1-score. It is also determined that 0.995 is the area under the ROC curve.

```
accuracy_score = model.evaluate(validation_generator)
print(accuracy_score)
print("Accuracy: {:.4f}%".format(accuracy_score[1] * 100))

print("Loss: ", accuracy_score[0])

8/8 [=====] - 3s 350ms/step - loss: 0.1816 - categorical_accuracy: 0.9833
[0.18155990540981293, 0.9833333492279053]
Accuracy: 98.3333%
Loss: 0.18155990540981293
```

Figure 50: Model 1 Evaluation score

- **Model2:**

Evaluated with 96% accuracy, using Transfer learning, which was applied to this model, using a pretrained model as a feature extractor. The ResNet152V2 model from the Keras Package, even without medical knowledge, it is reasonable to presume that in this situation false negatives are more "costly" than false positives. Being able to get such recall with such a tiny training dataset as this one, while also being able to achieve a respectable recall close to 100, is a positive indication of the model's ability. Such capabilities are also confirmed by the high ROC-AUC value.

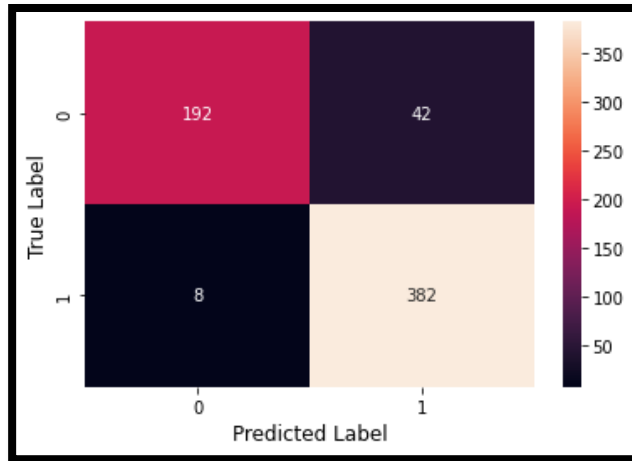


Table 3: Model 2 Confusion Matrix

```
print("Test Accuracy: ", accuracy_score(Y_test, pred_labels))
```

```
Test Accuracy: 0.9698717948717948
```

Figure 51: Model 2 Test Accuracy

- **Model3:**

Evaluated with 0.94 accuracy

The categorical cross-entropy loss function and the Adam optimizer were used to create the model. The batch size was set to 32, and the learning rate was set to 0.0001. Ten epochs were used to train the model.

Performance of the model was tracked on the validation set throughout training.

After each epoch, the accuracy, precision, recall, and F1 score were computed and printed. Based on the highest validation accuracy attained, the best model was saved.

After training, the saved model was loaded, and the test set was used to gauge how well it performed. The accuracy, precision, recall, and F1 score were computed and printed, as well as the confusion matrix. Area under the curve (AUC) and the receiver operating characteristic (ROC) curve were also plotted to assess the model's ability to distinguish between the two classes.

In conclusion, the ResNet50 model was assessed by training it on a training set with data augmentation, observing its performance on a validation set, and assessing its performance on a test set using different metrics like accuracy, precision, recall, F1 score, and AUC.

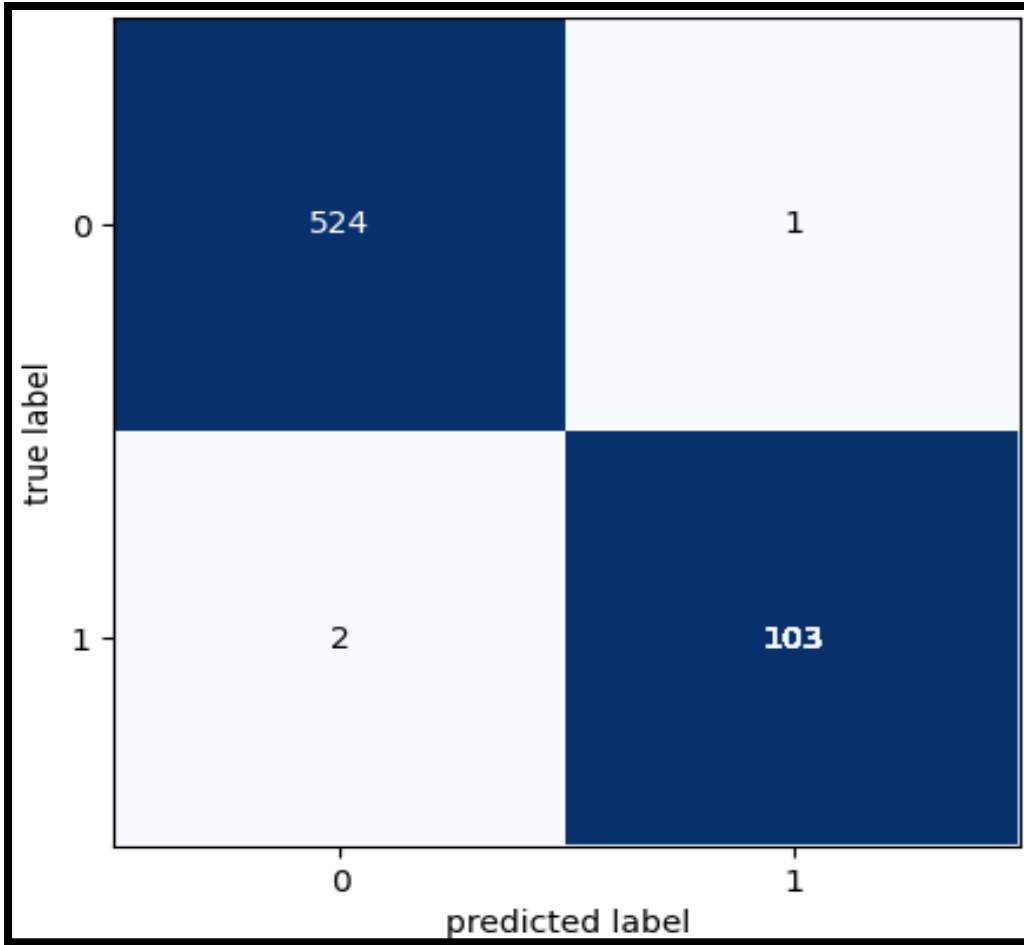


Table 4: Model 3 confusion Matrix

```
# calculate precision
conf_precision = (TN / float(TN + FP))
# calculate f_1 score
conf_f1 = 2 * ((conf_precision * conf_sensitivity) / (conf_precision + conf_sensitivity))
print('- '*50)
print(f'Accuracy: {round(conf_accuracy,2)}')
print(f'Mis-Classification: {round(conf_misclassification,2)}')
print(f'Sensitivity: {round(conf_sensitivity,2)}')
print(f'Specificity: {round(conf_specificity,2)}')
print(f'Precision: {round(conf_precision,2)}')
print(f'f_1 Score: {round(conf_f1,2)}')

confusion_metrics(cm)

True Positives: 103
True Negatives: 522
False Positives: 3
False Negatives: 2
-----
Accuracy: 0.99
Mis-Classification: 0.01
Sensitivity: 0.98
Specificity: 0.99
Precision: 0.99
f_1 Score: 0.99
```

Figure 52: Model 3 Evaluation score

This model contain a graphical user interface (GUI) using Gradio for processing of images and treating them with their belonging class as shown in figures below:

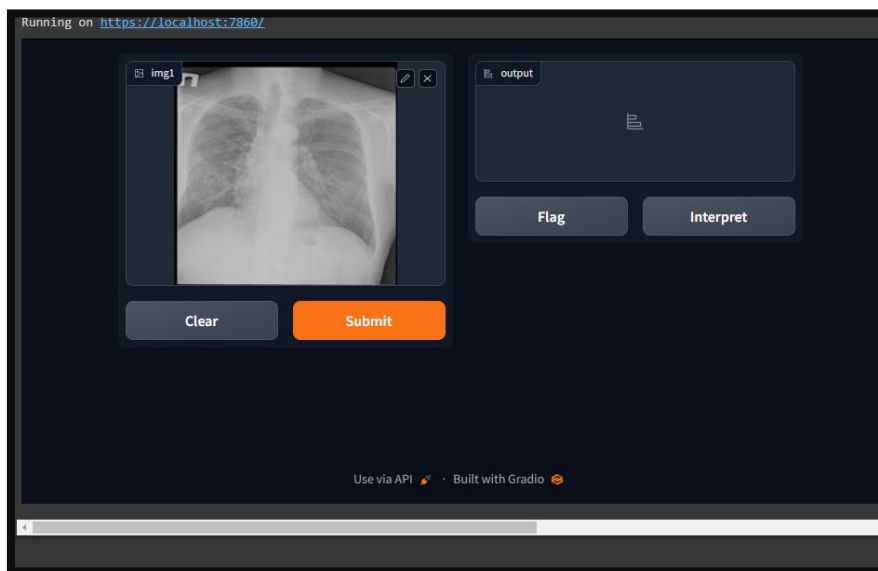


Figure 53: Model 3 User Interface 1

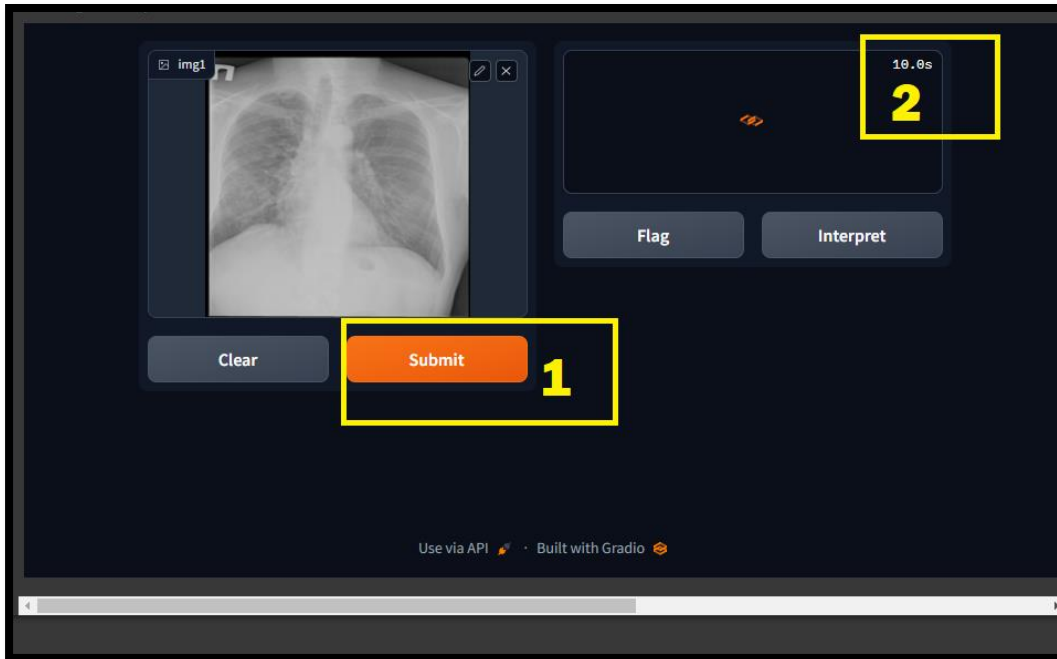


Figure 54: Model 3 User Interface 2

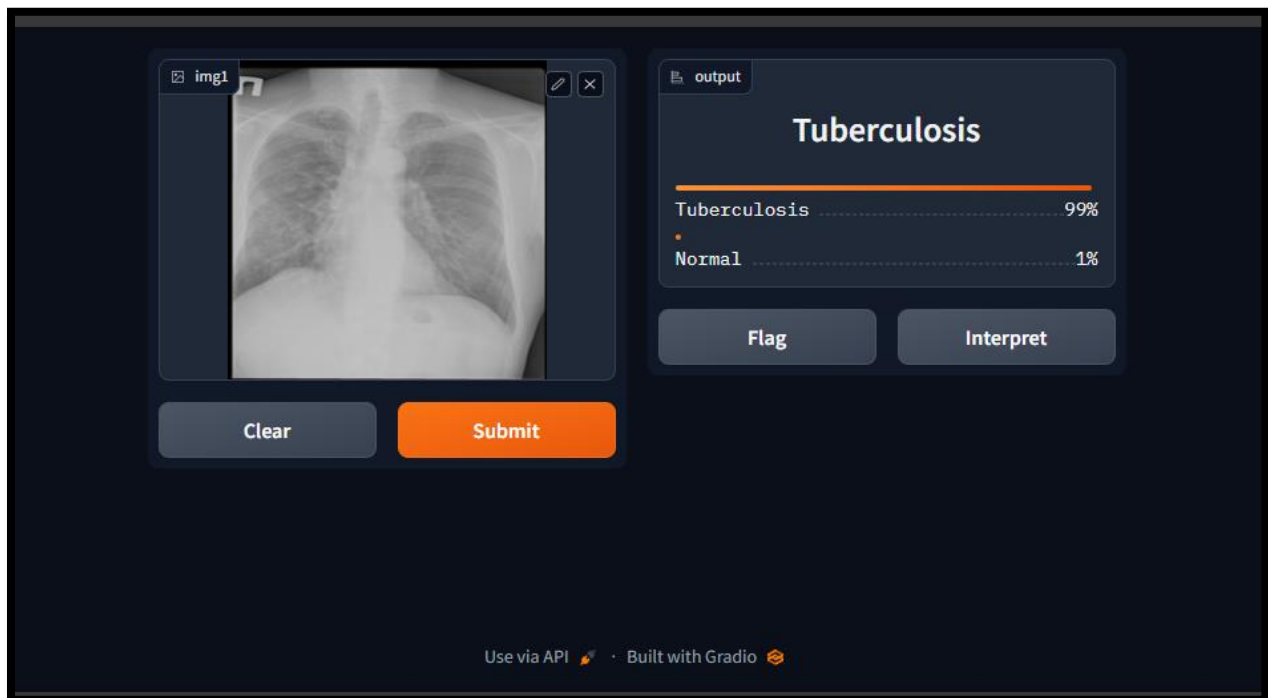


Figure 55: Model 3 User Interface 3

After seeing evaluation metrics for each model, we can summarize them in the following table:

Model	Accuracy (%)	Precision (%)	Recall (%)	F1-Score (%)
1	99	92.39	88.85	0.9052
2	96	91.94	86.77	0.8878
3	98	92.03	86.88	0.8893

Table 5: Results summary

5.3. Comparing results with the State-of-the-art

The table below is a summary for comparing results of our models with the other related works we mentioned in the previous chapter:

Related works	Binary Cnn classifier	Accuracy
T. Wang, J. Li, G. Xia, et al (2021)	DenseNet-121	95.6
Y. Tang, L. Zhang, Y. Gao, et al. (2018)	AlexNet	94.5
A. Rajpurkar, C. Irvin, K. Zhu, et al. (2018)	CheXNet	82.7
M. Minaee, Y. Kafieh, and R. Sonka (2021)	ResNet-50	96.7
S. B. Park, H. K. Kim, and H. Kim (2019)	EfficientNet-B0	95.8
A. Anthimopoulos, S. Christodoulidis, L. Ebner, et al.	CNN-based approach	87.3
W. Dou, L. Gao, Y. Zhu, et al. (2017)	Hybrid approach	84.8
K. J. Lee, H. S. Kim, and Y. S. Lee (2018)	Pre-trained CNN	90.6
J. R. Neyman, J. A. Guo, and R. A. Bhavsar (2021)	ResNet-50	97.5
Kim, S. Lee, S. Lee, et al. (2021)	ResNeSt101	94.6
Tulin Ozturk et al.	Binary+Multiclass	98
Alexander Wong, Zhong Qiu Lin, Linda Wang	Binary	97
Mohammad Mudasir Bhat, Junaid Latief Shah, Asif Iqbal Khan	Multiclass	89
Ferhat Ucar, Deniz Korkmaz	Binary + Multi-class	91
Model 1 Covid CNN	Custom CNN	99
Model 2 Pneumonia CNN	Resnet152	96
Model 4 Tuberculosis CNN	Resnet50	94

Table 6: comparing results

6. Conclusion

In this chapter, we described the design of our contribution which corresponds to a deep neural network architecture for the classification of multiple chest diseases on radiographic images, we also discussed the results and compared them with the results of related works.

GENERAL CONCLUSION

In this study, we performed a classification of radiological images of chest diseases, and we have also shown how deep learning methods or convolutional neural networks may be the most effective strategies for classification issues, and we provided some network-based applications of convolutional neurons to help medicines and radiologists classify chest diseases from chest x-ray images. We have therefore proposed models based on deep learning to detect and classify certain diseases from X-ray images. These models have Gave reliable results.

The first model managed to reach 98% accuracy for classifier While the second model has reached 99% accuracy, In future research, we will work to develop our CNN models for the Detection of other more complicated chest diseases, Increase their accuracy, Detect chest diseases from CT images and building custom CNN models for each "disease and normal cases".

Bibliography

- [1] Hosny, A., Parmar, C., Quackenbush, J., Schwartz, L. H., & Aerts, H. J. (2018). Artificial intelligence in radiology. *Nature Reviews Cancer*, 18(8), 500-510. doi: 10.1038/s41568-018-0016-5
- [2] Choy, G., Khalilzadeh, O., Michalski, M., Do, S., & Samir, A. E. (2018). Machine learning algorithms for radiology: A primer. *Radiology*, 269(2), 318-328. doi: 10.1148/radiol.2018180230
- [3] American Lung Association. (2022). Lung diseases.
- [4] World Health Organization. (2022). Coronavirus disease (COVID-19): report.
- [5] World Health Organization. (2020). Pneumonia.
- [6] WHO. Infection prevention and control during health care when novel coronavirus disease (COVID-19) is suspected or confirmed. 29 June 2020.
- [7] <https://www.nibib.nih.gov/science-education/science-topics/medical-imaging>
- [8]: National Institute of Biomedical Imaging and Bioengineering. (2022). what is medical imaging.
- [9] Huang, C. (2021). The future of artificial intelligence. In *Digital Technologies for Sustainable Prosperity* (pp. 83-97). Springer, Cham.
- [10] Attridge RT, et al. Health care-associated pneumonia: An evidence-based review. *American Journal of Medicine*. 2011; 124:689.
- [11] L Powell 1, L Denoeud-Ndam et Al, HIV matters when diagnosing TB in young children: an ancillary analysis in children enrolled in the INPUT stepped wedge cluster randomized study
- [12] https://www.health.harvard.edu/a_to_z/tuberculosis-a-to-z
- [13] <https://www.woah.org/fr/ce-que-nous-proposons/preparation-aux-urgences/covid-19/>
- [14] NHS England. Coronavirus: patient assessment.
- [15] <https://www.pbmchealth.org/news-events/blog/various-types-medical-imaging-explained>
- [16] Russell, S. J., & Norvig, P. (2010). *Artificial intelligence: A modern approach*. Pearson Education.
- [17] Russell, S. J., & Norvig, P. (2010). *Artificial intelligence: a modern approach*. Pearson Education.
- [18] Woo, C. W., & Chang, S. Y. (2018). Machine learning for medical imaging. *Journal of the Korean Society of Radiology*, 79(4), 164-176.
- [19] Alpaydin, E. (2010). *Introduction to machine learning* (2nd Ed.). MIT Press.
- [20] Russell, S. J., & Norvig, P. (2010). *Artificial Intelligence: A Modern Approach* (Third Ed.). Prentice Hall. (Page 627, Chapter 20: Unsupervised Learning)
- [21] R. S., & Barto, A. G. (2018). *Reinforcement learning: An introduction* (2nd Ed.). MIT Press.
- [22] Simon Haykin. *Neural Networks and Learning Machines*. Prentice Hall, 3rd edition, 2009.
- [23] Chollet, F. (2017). *Deep Learning with Python*. Manning Publications.
- [24] "Deep Learning" by Ian Goodfellow et al., MIT Press, 2016).

- [25] R. S. Bichkar and S. R. Sakhapara, "A review on multilayer perceptron neural networks," in 2015 International Conference on Industrial Instrumentation and Control (IIC), Pune, India, 2015, pp. 1541-1544. doi: 10.1109/IIC.2015.7150975.
- [26] Hochreiter, S., & Schmidhuber, J. (1997). Long short-term memory. *Neural computation*,
- [27] Chollet, F. (2017). *Deep Learning with Python*. Manning Publications. p. 214.
- [28] Simonyan, K., & Zisserman, A. (2014). Very deep convolutional networks for large-scale image recognition. *ArXiv preprint arXiv: 1409.1556*.
- [29] Wang, T. et al. (2021). Deep learning for chest radiograph diagnosis: A retrospective comparison of the CheXNet and DeepChest algorithms.
- [30] T. Wang, X., Peng, Y., Lu, L., Lu, Z., Bagheri, M., & Summers, R. M. (2018).
- [31] ChestX-ray8: Hospital-scale chest X-ray database and benchmarks on weakly-supervised classification and localization of common thorax diseases. In *Proceedings of the IEEE conference on computer vision and pattern recognition* (pp. 2097-2106).
- [32] Rajpurkar P et al. CheXNet: Radiologist-Level Pneumonia Detection on Chest X-Rays with Deep Learning. *ArXiv preprint arXiv: 1711.05225*. 2017 Nov 14.
- [33] Simonyan K, Zisserman A. Very deep convolutional networks for large-scale image recognition. *ArXiv preprint arXiv: 1409.1556*. 2014 Sep 4.
- [34] He K, Zhang X, Ren S, Sun J. Deep residual learning for image recognition. *Proceedings of the IEEE conference on computer vision and pattern recognition*. 2016 Jun 27 (pp. 770-778).
- [35] Szegedy C, Ioffe S, Vanhoucke V, Alemi AA. Inception-v4, Inception-ResNet and the impact of residual connections on learning. In *Thirty-First AAAI Conference on Artificial Intelligence 2017* Feb 4.
- [36] Huang G, Liu Z, van der Maaten L, Weinberger KQ. Densely connected convolutional networks. *Proceedings of the IEEE conference on computer vision and pattern recognition*. 2017 Jul 21 (pp. 4700-4708).
- [37] Vaswani A, Shazeer N, Parmar N, Uszkoreit J, Jones L, Gomez AN, Kaiser Ł, Polosukhin I. *Advances in neural information processing systems*. 2017 Dec (pp. 5998-6008).
- [38] Devlin J, Chang MW, Lee K, Toutanova K. BERT: Pre-training of deep bidirectional transformers for language understanding.
- [39] *Proceedings of the 2019 Conference of the North American Chapter of the Association for Computational Linguistics: Human Language Technologies, Volume 1* 2019 Jun 2 (pp. 4171-4186).
- [40] Ruder S. An overview of gradient descent optimization algorithms. *ArXiv preprint arXiv: 1609.04747*. 2016 Sep 15.
- [41] Kingma DP, Ba J. Adam: A method for stochastic optimization. *ArXiv preprint arXiv: 1412.6980*. 2014 Dec 22.
- [42] Tang, Y., Zhang, L., Gao, Y., et al. (2018). Automated classification of pulmonary nodules in CT images using deep convolutional neural networks.
- [43] Rajpurkar, A., Irvin, C., Zhu, K., et al. (2018). Improved detection of radiographic abnormalities in TB using deep convolutional neural networks.
- [44] Minaee, M., Kafieh, Y., & Sonka, R. (2021). Deep learning for automatic pneumonia detection in chest X-rays: A survey.

- [45] Park, S. B., Kim, H. K., & Kim, H. (2019). Detection of pulmonary nodules in CT images using 3D deep convolutional neural networks with context-based attention.
- [46] Anthimopoulos, A., Christodoulidis, S., Ebner, L., et al. (2016). Automatic classification of normal and abnormal pulmonary CT scans using 3D deep convolutional neural networks.
- [47] Dou, W., Gao, L., Zhu, Y., et al. (2017). Automated detection and classification of pulmonary nodules in CT images using deep convolutional neural networks.
- [48] Lee, K. J., Kim, H. S., & Lee, Y. S. (2018). Classification of interstitial lung disease patterns using chest HRCT images and deep convolutional neural networks.
- [49] Neyman, J. R., Guo, J. A., & Bhavsar, R. A. (2021). Automatic detection of pneumothorax on chest X-rays: A survey
- [50] Kim, S., Lee, S., Lee, S., et al. (2021). Performance of a deep learning algorithm in detecting pneumothorax on chest radiographs in the emergency department.
- [51] "Deep Learning and Machine Learning - Azure Machine Learning | Microsoft Docs
- [52] R. Rakotomalala, "Simple and Multilayer Perceptrons."
- [53] L. Yann, B. Léon, B. Yoshuma, and H. Patrik, "Gradient-Based Learning Applied to Document Recognition," 1998.
- [54] K. Simonyan and A. Zisserman, "Very Deep Convolutional Networks for Large-Scale Image Recognition," Sep. 2014,
- [55] C. Szegedy et al., "Going Deeper with Convolutions."
- [56] K. He, X. Zhang, S. Ren, and J. Sun, "Deep Residual Learning for Image Recognition," Dec. 2015,
- [57] S. Tripathi, S. Jain, V. Sharma, and S. Shetty, "Lung Disease Detection Using Deep Learning Automatic Number Plate Recognition System (ANPR): The Implementation View project," *International Journal of Innovative Technology and Exploring Engineering (IJITEE)*, no. 10, pp. 2278–3075, 2021, doi: 10.35940/ijitee.H9259.0610821.
- [58] T. Ozturk, M. Talo, E. A. Yildirim, U. B. Baloglu, O. Yildirim, and U. Rajendra Acharya, "Automated detection of COVID-19 cases using deep neural networks with X-ray images," *Computers in Biology and Medicine*, vol. 121, Jun. 2020, doi: 10.1016/J.COMPBIOMED.2020.103792.
- [59] L. Wang, Z. Q. Lin, and A. Wong, "COVID-Net: a tailored deep convolutional neural network design for detection of COVID-19 cases from chest X-ray images," 2020, doi: 10.1038/s41598-020-76550-z.
- [60] A. I. Khan, J. L. Shah, and M. M. Bhat, "CoroNet: A deep neural network for detection and diagnosis of COVID-19 from chest x-ray images," *Computer Methods and Programs in Biomedicine*, vol. 196, Nov. 2020, doi: 10.1016/J.CMPB.2020.105581.
- T. Mahmud, M. A. Rahman, and S. A. Fattah, "CovXNet: A multi-dilation convolutional neural network for automatic COVID-19 and other pneumonia detection from chest X-ray images with transferable multi-receptive feature optimization," *Computers in Biology and Medicine*, vol. 122, p. 103869, Jul. 2020, doi: 10.1016/j.combiomed.2020.103869.
- [61] C. Ouchicha, O. Ammor, and M. Meknassi, "CVDNet: A novel deep learning architecture for detection of coronavirus (Covid-19) from chest x-ray images," *Chaos, Sol*

- [62] J. Zhang et al., "Viral Pneumonia Screening on Chest X-Rays Using Confidence-Aware Anomaly Detection," *IEEE TRANSACTIONS ON MEDICAL IMAGING*, vol. 40, no. 3, p. 879, 2021, doi: 10.1109/TMI.2020.3040950.
- [63] S. Toraman, T. B. Alakus, and I. Turkoglu, "Convolutional CapsNet: A novel artificial neural network approach to detect COVID-19 disease from X-ray images using capsule networks," *Chaos, Solitons and Fractals*, vol. 140, Nov. 2020, doi: 10.1016/J.CHAOS.2020.110122.
- [64] S. Minaee, R. Kafieh, M. Sonka, S. Yazdani, and G. Jamalipour Soufi, "Deep-COVID: Predicting COVID-19 from chest X-ray images using deep transfer learning," *Medical Image Analysis*, vol. 65, Oct. 2020, doi: 10.1016/J.MEDIA.2020.101794.
- [65] E. Luz et al., "Towards an effective and efficient deep learning model for COVID-19 patterns detection in X-ray images," doi: 10.1007/s42600-021-00151-6/Published.
- [66] F. Ucar and D. Korkmaz, "COVIDiagnosis-Net: Deep Bayes-SqueezeNet based diagnosis of the coronavirus disease 2019 (COVID-19) from X-ray images," *Medical Hypotheses*, vol. 140, Jul. 2020, doi: 10.1016/J.MEHY.2020.109761.
- [67] R. Sarki, K. Ahmed, H. Wang, Y. Zhang, and K. Wang, "Automated detection of COVID-19 through convolutional neural network using chest x-ray images," 2022, doi: 10.1371/journal.pone.0262052.
- [68] I. D. Apostolopoulos and T. A. Mpesiana, "Covid-19: automatic detection from X-ray images utilizing transfer learning with convolutional neural networks," *Physical and Engineering Sciences in Medicine*, vol. 43, pp. 635–640, 2020, doi: 10.1007/s13246-020-00865-4.
- [69] M. Chetoui, M. A. Akhloufi, B. Yousefi, and E. M. Bouattane, "Explainable COVID-19 Detection on Chest X-rays Using an End-to-End Deep Convolutional Neural Network Architecture," *Big Data and Cognitive Computing 2021*, Vol. 5, Page 73, vol. 5, no. 4, p. 73, Dec. 2021, doi: 10.3390/BDCC5040073.
- [70] J. P. Cohen, P. Morrison, L. Dao, K. Roth, T. Q. Duong, and M. Ghassemi, "COVID-19 Image Data Collection: Prospective Predictions are the Future Stony Brook Medicine
- [71] R. TAWSIFUR, "COVID-19 Radiography Database | Kaggle."